iScience

CellPress

Article

A Glial-Neuronal Circuit in the Median Eminence Regulates Thyrotropin-Releasing Hormone-Release via the Endocannabinoid System

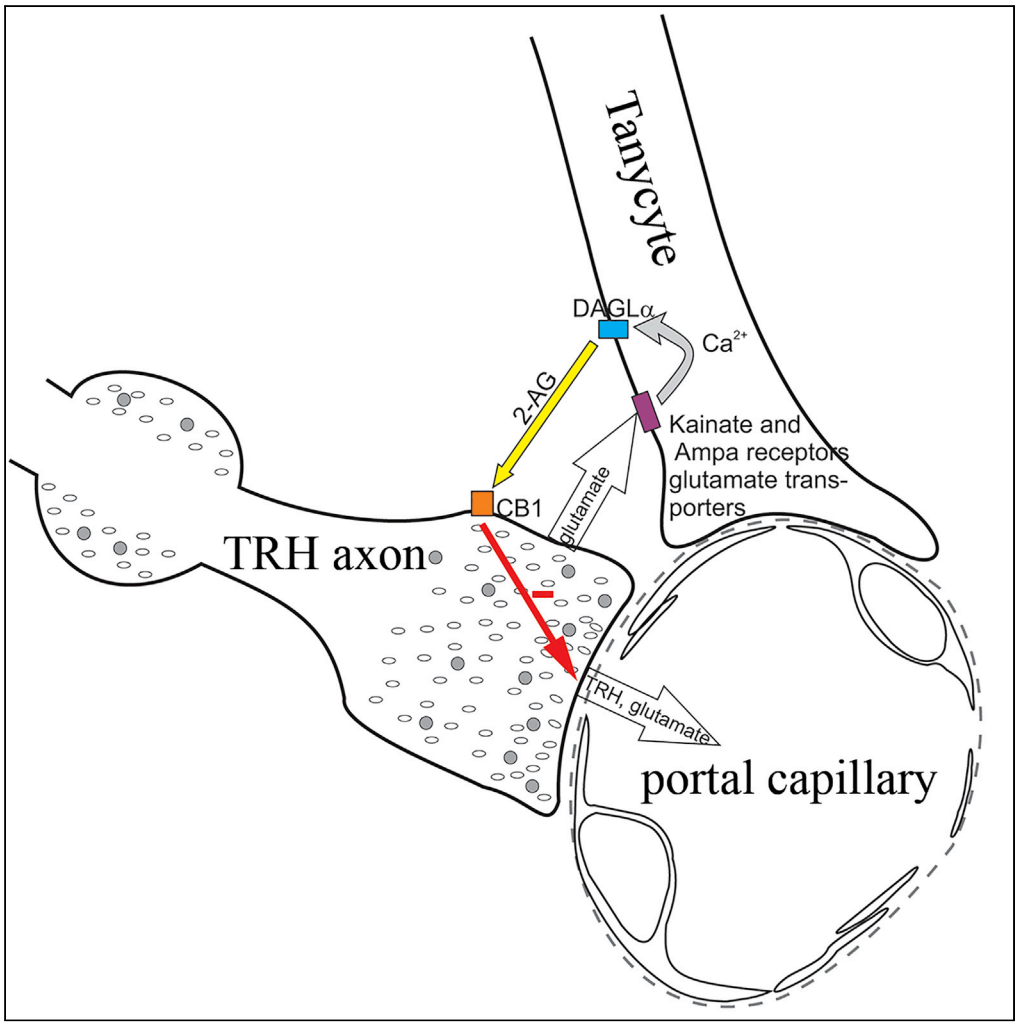

Erzsébet Farkas, Edina Varga, Balázs Kovács, ..., Jean-Louis Charli, Patricia Joseph-Bravo, Csaba Fekete

fekete.csaba@koki.mta.hu

HIGHLIGHTS

Tanycytes tonically inhibit the activity of TRH axons via endocannabinoid release

Glutamate depolarizes the tanycytes and regulates their 2-AG synthesis

Glutamate released from the hypophysiotropic TRH axons influences tanycytes

A microcircuit utilizing glutamate and endocannabinoids regulates TRH release

Farkas et al., iScience *23*, 100921
March 27, 2020
https://doi.org/10.1016/j.isci.2020.100921

iScience

CellPress

Article

A Glial-Neuronal Circuit in the Median Eminence Regulates Thyrotropin-Releasing Hormone-Release via the Endocannabinoid System

Erzsébet Farkas,[1,15] Edina Varga,[1,15] Balázs Kovács,[1,15] Anett Szilvásy-Szabó,[1,15] Antonieta Cote-Vélez,[2] Zoltán Péterfi,[1] Magdalini Matziari,[3] Mónika Tóth,[1] Dóra Zelena,[4,5] Zsolt Mezriczky,[6] Andrea Kádár,[1] Dóra Kővári,[1] Masahiko Watanabe,[7] Masanobu Kano,[8] Ken Mackie,[9] Balázs Rózsa,[10] Yvette Ruska,[1] Blanka Tóth,[11] Zoltán Máté,[12] Ferenc Erdélyi,[12] Gábor Szabó,[12] Balázs Gereben,[1] Ronald M. Lechan,[13,14] Jean-Louis Charli,[2] Patricia Joseph-Bravo,[2] and Csaba Fekete[1,14,16,*]

SUMMARY

Based on the type-I cannabinoid receptor (CB1) content of hypophysiotropic axons and the involvement of tanycytes in the regulation of the hypothalamic-pituitary-thyroid (HPT) axis, we hypothesized that endocannabinoids are involved in the tanycyte-induced regulation of TRH release in the median eminence (ME). We demonstrated that CB1-immunoreactive TRH axons were associated to DAGLα-immunoreactive tanycyte processes in the external zone of ME and showed that endocannabinoids tonically inhibit the TRH release in this tissue. We showed that glutamate depolarizes the tanycytes, increases their intracellular Ca^{2+} level and the 2-AG level of the ME via AMPA and kainite receptors and glutamate transport. Using optogenetics, we demonstrated that glutamate released from TRH neurons influences the tanycytes in the ME.

In summary, tanycytes regulate TRH secretion in the ME via endocannabinoid release, whereas TRH axons regulate tanycytes by glutamate, suggesting the existence of a reciprocal microcircuit between tanycytes and TRH terminals that controls TRH release.

INTRODUCTION

Tanycytes are specialized glial cells lining the floor and lateral walls of the third ventricle behind the optic chiasm (Rodriguez et al., 2005; Prevot et al., 2018). The small cell bodies of these cells form the ventricular wall, whereas their long basal processes project into the median eminence (ME) or into the neuropil of the arcuate, ventromedial, and dorsomedial hypothalamic nuclei (Rodriguez et al., 2005; Prevot et al., 2018).

In the external zone of the ME, tanycyte processes terminate around the fenestrated capillaries of the hypophysial portal circulation and intermingle with the terminals of hypophysiotropic axons, suggesting that the tanycytes (β2 tanycytes) that project to the ME may be involved in the regulation of the neurohypophysial systems (Rodriguez et al., 2005; Prevot et al., 2018). Indeed, a major role of tanycytes has been demonstrated in the regulation of the hypothalamic-pituitary-thyroid (HPT) axis by multiple mechanisms (Lechan and Fekete, 2007; Rodriguez-Rodriguez et al., 2019). As tanycytes are the primary hypothalamic cell types that express the thyroid hormone activating enzyme, type 2 deiodinase (D2), these cells can regulate the activity of hypophysiotropic thyrotropin-releasing hormone (TRH) synthesizing neurons by controlling the hypothalamic availability of T3, the active form of thyroid hormones that can effectively bind to the nuclear receptors and suppresses TRH release (Fekete and Lechan, 2014). For example, endotoxin-induced increase of tanycyte D2 activity has a critical role in the development of central hypothyroidism (nonthyroidal illness syndrome) (Fekete et al., 2005; Freitas et al., 2010). Tanycytes also express the TRH-degrading ectoenzyme (TRH-DE) (Sanchez et al., 2009), providing a mechanism by which they can control the amount of TRH reaching the pituitary by degrading the tripeptide in the extracellular space of the external zone of the ME.

We recently observed that large number of hypophysiotropic axon terminals in the external zone of the ME contain type 1 cannabinoid receptor (CB1) (Wittmann et al., 2007), raising the possibility that endocannabinoids may also regulate the release of hypophysiotropic hormones in the ME. In most cases, endocannabinoids are released from postsynaptic neurons and act on CB1 receptors located on presynaptic axon

[1]Department of Endocrine Neurobiology, Institute of Experimental Medicine, Szigony u. 43, Budapest 1083, Hungary

[2]Departamento de Genética del Desarrollo y Fisiología Molecular, Instituto de Biotecnología, Universidad Nacional Autónoma de México (UNAM), Cuernavaca 62210, México

[3]Department of Chemistry, Xi'an Jiaotong-Liverpool University, Suzhou, Jiangsu 215123, China

[4]Department of Behavioral Neurobiology, Institute of Experimental Medicine, Budapest, Hungary

[5]Centre for Neuroscience, Szentágothai Research Centre, Institute of Physiology, Medical School, University of Pécs, Pécs 7624, Hungary

[6]Faculty of Information Technology and Bionics, Pázmány Péter Catholic University, Budapest 1088, Hungary

[7]Department of Anatomy, Hokkaido University School of Medicine, Sapporo 060-8638, Japan

[8]Department of Neurophysiology, Graduate School of Medicine, The University of Tokyo, Tokyo 113-0033, Japan

[9]Gill Center for Biomolecular Science, Department of Psychological and Brain Sciences, Indiana University, Bloomington 474052, IN, USA

[10]Laboratory of 3D Functional Network and Dendritic Imaging, Institute of

Continued

terminals (Piomelli, 2003; Kano et al., 2009). The external zone of the ME houses very few neuronal perikarya, and endocannabinoids can travel only very short distances in the brain (Regehr et al., 2009) supporting a glial origin of endocannabinoids in this brain region. Therefore, we hypothesized that tanycytes, the most abundant glial cell type of the ME, may control the release of hormones, including TRH, from the hypophysiotropic axon terminals of the ME via the endocannabinoid system. In addition to TRH, hypophysiotropic TRH axons also release glutamate (Hrabovszky et al., 2005). Since tanycytes express glutamate receptors (Eyigor and Jennes, 1998; Kawakami, 2000), and glutamate is known to regulate endocannabinoid synthesis and release (Katona et al., 2006), we further hypothesized that glutamate release from hypophysiotropic axon terminals signal toward the tanycytes, establishing a local regulatory microcircuit between TRH axons and tanycytes in the external zone of the ME.

To test these hypotheses, we determined whether the tanycytes can control the release of TRH from hypophysiotropic terminals in the ME by utilizing the endocannabinoid system and whether glutamate released from axon terminals of hypophysiotropic TRH neurons regulates β-tanycytes of the ME.

RESULTS

Expression of CB1 in Hypophysiotropic TRH Neurons of Mice

To determine whether the hypophysiotropic TRH neurons express the CB1 receptor, double-labeling *in situ* hybridization was performed. CB1 mRNA was observed in the majority of neurons in the hypothalamic paraventricular nucleus (PVN) where the perikaryon of the hypophysiotropic TRH neurons reside; however, the intensity of the hybridization signal was much lower than that observed in cortical or hippocampal areas. Analyses of the double-labeled sections showed that silver grains denoting CB1 mRNA were observed above 73.4 $\pm$ 1.5% of the TRH neurons in the PVN (Figure 1A). In addition, double-labeling immunofluorescence showed that punctuate CB1-immunoreactive signal was present in the majority of TRH-IR axon varicosities in the external zone of the ME suggesting that the hypophysiotropic TRH axons are sensitive to endocannabinoid signaling (Figure 1B).

DAGLα-Immunoreactivity Is Present in Tanycytes in the ME and Associated with CB1-IR TRH Axons in Mice

To determine the cell type that releases endocannabinoids in the ME, the localization of diacylglycerol lipase α (DAGLα), the synthesizing enzyme of one of the main endocannabinoids, 2-arachinodonoylglycerol (2-AG), was studied. At light microscopic level, DAGLα-immunoreactivity was observed in tanycyte cell bodies lining the floor (β2 tanycytes) and the lateral evagination (β1 tanycytes) of the third ventricle (Figure 1C). In addition, DAGLα-immunoreactivity was also observed in processes running toward the capillary plexus of the external zone of the ME (Figure 1D), reminiscent of the distribution of the β-tanycyte basal processes. Colocalization of DAGLα-immunoreactivity and the ZsGreen fluorescence in Rax/CreERT2//Gt(ROSA)26Sor_CAG/LSL_ZsGreen1 mice where the green fluorescence labels the tanycytes (Pak et al., 2014) demonstrate that DAGLα is indeed present in tanycytes (Figure 1E).

Immunoelectron microscopy also demonstrated DAGLα immunoreactivity to be present in tanycyte cell bodies and processes in the ME. In the external zone of the ME, DAGLα-IR endfeet processes of β2-tanycytes were closely associated with axon terminals of hypophysiotropic neurons (Figures 1F and 1G). Triple-labeling immunofluorescence demonstrated that axon terminals containing both TRH immunoreactivity and punctate immunofluorescence labeling the CB1 immunoreactivity are closely associated to DAGLα-IR tanycyte processes (Figure 1H).

Endocannabinoids Tonically Inhibit TRH Release from the ME in Rats

To determine whether endocannabinoids affect basal TRH release, ME explants were treated with the CB1 antagonist, AM251, or CB1 agonist, WIN55,212-2, in the presence of a TRH-degrading enzyme (TRH-DE) inhibitor. AM251 stimulated TRH release causing an approximately 2-fold increase in the TRH concentration of the ME explant supernatant ($p < 0.05$; Figure 2A). The CB1 agonist, however, had no effect ($p = 0.48$; Figure 2A). To test the hypothesis that the exogenous CB1 agonist was ineffective because of saturation of CB1 by its endogenous ligand, the effect of WIN55,212-2 was tested in the presence of the DAGLα inhibitor, tetrahydrolipstatin (THL). Treatment of the explants with THL caused an increase in TRH release ($p < 0.01$), whereas the CB1 agonist decreased THL-induced TRH release ($p < 0.05$; Figure 2B).

Experimental Medicine, Budapest 1083, Hungary

[11]Department of Inorganic and Analytical Chemistry, Budapest University of Technology and Economics, Szent Gellert ter 4, Budapest 1111, Hungary

[12]Medical Gene Technology Unit, Institute of Experimental Medicine, Budapest 1083, Hungary

[13]Department of Medicine, Division of Endocrinology, Diabetes and Metabolism, Tupper Research Institute, Tufts Medical Center, Boston 02111, MA, USA

[14]Department of Neuroscience, Tufts University School of Medicine, Boston 02111, MA, USA

[15]These authors contributed equally

[16]Lead contact

*Correspondence: fekete.csaba@koki.mta.hu

https://doi.org/10.1016/j.isci.2020.100921

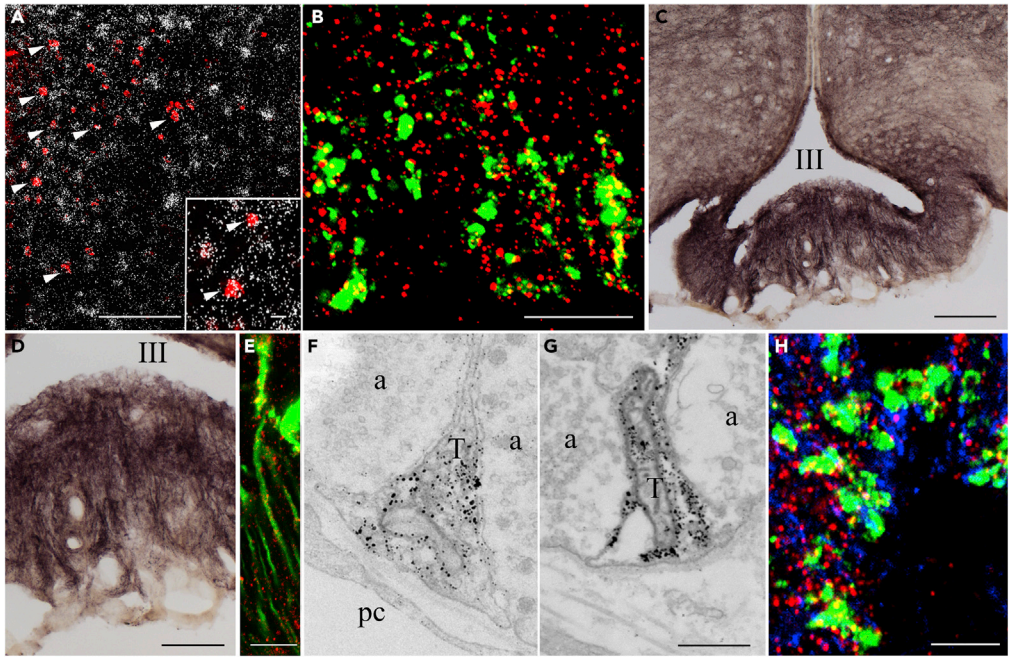

Figure 1. Elements of the Endocannabinoid System Are Present in the Hypophysiotropic TRH Neurons and in the Tanycytes in the External Zone of the ME

(A) Double-labeling *in situ* hybridization demonstrates that the majority of TRH neurons (red) in the PVN express CB1 mRNA labeled by the presence of silver grains. Arrowheads point to double-labeled neurons expressing both TRH and CB1 mRNAs. Inset illustrates double-labeled neurons at higher magnification (arrowheads).

(B) Double-labeling immunocytochemistry demonstrates the presence of CB1 immunoreactivity (red dots) in TRH-IR hypophysiotropic axon varicosities (green) in the external zone of the ME. The CB1 immunoreactivity within the TRH axons appear yellow owing to the color mixing.

(C) High level of DAGLα immunoreactivity is present in tanycyte cell bodies lining the floor of the third ventricle and the wall of the lateral evaginations. Dense DAGLα-IR fiber network is also present in the median eminence.

(D) Higher-magnification image illustrates that the DAGLα-IR fibers run perpendicular to the surface of the median eminence.

(E) DAGLα immunofluorescence (red) in tanycyte processes where the green fluorescent protein labels the tanycytes. The spotted DAGLα immunofluorescence can be observed along the tanycyte processes.

(F and G) Ultrastructural images demonstrate that the DAGLα immunoreactivity (labeled by silver grains) is present in tanycyte endfeet processes terminating around portal capillaries.

(H) The CB1-containing (red) TRH-IR (green) axon varicosities are closely associated to DAGLα-IR (blue) tanycyte processes.

Scale bars, 100 μm in (A) and (C), 10 μm in inset and (B), 50 μm in (D), 10 μm in (E), 0.5 μm in (G) that corresponds to (F) and (G), and 5 μm in (H). Abbreviations: III, third ventricle; a, axon varicosity; pc, portal capillary; T, tanycyte endfeet. See also Figure S1.

These data demonstrate that endocannabinoids inhibit TRH release in the ME and there is a tonic, endocannabinoid-induced inhibition of TRH release in the ME explants.

β2-Tanycytes Express Glutamate Receptors and Glutamate Transporters in Mice

To determine whether glutamate and TRH released from the hypophysiotropic TRH axons influence β2-tanycytes, the expression of the glutamate receptor subunits, glutamate transporters, and TRH receptors was studied in β2-tanycyte cell bodies isolated by laser capture microdissection (Table 1). A high level of SLC1A3 (EAAC1/EAAT3) glutamate transporter mRNA and low level of SLC1A1 (GLAST/EAAT1) and SLC1A2 (GLT-1/EAAT2) mRNA was detected in β-tanycytes, whereas SLC1A6 (EAAT4) and SLC1A7 (EAAT5) glutamate transporters were not expressed.

Among the AMPA receptor subunits, mRNA of GRIA1 and GRIA2 was observed. GRIK3 was the kainite subunit with the highest expression, followed by GRIK2,4,5 that, although low, was still detectable. GRIN3A was the only NMDA receptor subunit and GRM4 the only metabotropic glutamate receptor detected in

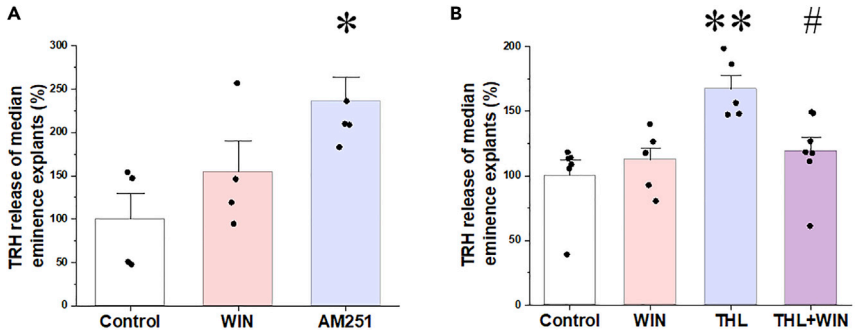

Figure 2. Effects of Pharmacological Manipulation of the Endocannabinoid System on TRH Release from Median Eminence Explants

(A) TRH recovered from median eminence explants incubated in ACSF containing the TRH-DE inhibitor, P-TRH (200 nM), was measured by RIA. WIN 55,212-2 (1 μM; N = 4) had no effect on the TRH release of the median eminence explants, whereas AM251 (1 μM; N = 5) induced a 2-fold increase of TRH release ($N_{Control}$ = 4).

(B) To determine whether the absence of CB1 agonist effect is due to saturation of CB1 by endogenous cannabinoids in the explants, the DAGLα inhibitor tetrahydrolipstatin (THL) was used to inhibit endocannabinoid synthesis. THL caused a marked increase of TRH release (N = 5). Although WIN 55,212-2 alone had no effect on TRH release (N = 6), it significantly decreased TRH release when 2-AG synthesis was blocked by THL (N = 7) indicating that a tonic endocannabinoid release inhibits TRH release from axons of the median eminence ($N_{Control}$ = 6). Data are presented as percentage of control group and as mean ± SEM (N = 5). Data were analyzed by one-way ANOVA and Tukey post hoc test. * significantly different from control, *$p < 0.05$, **$p < 0.01$; # significantly different from THL treated group ($p < 0.05$). The amount of TRH released during 2 × 10 min by the control groups was 80 ± 4 pg and residual intracellular TRH was 1860 ± 40 pg/2 ME explants. There was no difference in residual intracellular TRH between control and drug-treated groups. Abbreviations: WIN, WIN55,212-2; THL, tetrahydrolipstatine.

β2-tanycytes, but both had relatively low expression level. Expression of TRH receptors was not detected in the β2-tanycytes.

These data suggest that glutamate effects on β2-tanycytes occur primarily via AMPA and kainate receptors and the glutamate transporter, SLC1A3.

Glutamate Induces Depolarization of the Membrane Potential of β2-Tanycytes in Mice

To elucidate the effect of glutamate on the β2-tanycytes, patch clamp electrophysiology was performed. The membrane potential of the β2-tanycytes was −77.52 ± 0.47 mV (n = 83) under control conditions. Four different glutamate concentrations were applied to the cells, each causing dose-dependent depolarization of β2-tanycytes (glutamate treatments induced change of membrane potential: control: 0.25 ± 0.42 mV, n = 6; 250 μM: 4.29 ± 0.46 mV, n = 11, $p = 0.038$; 500 μM: 7.53 ± 0.99 mV, n = 12, $p < 0.001$; 750 μM: 8.59 ± 0.94 mV, n = 8, $p < 0.001$; and 1,000 μM: 6.85 ± 0.83 mV, n = 6, $p < 0.001$; Figure 3A). Treatment with 250 μM glutamate caused a significant depolarization, but significantly less than the treatment with 500 μM glutamate ($p = 0.049$). As 500 μM had similar effect as that of 750 and 1,000 μM concentrations, 500 μM was selected for further studies.

To exclude the possibility that the effect of glutamate was mediated by tetrodotoxin (TTX; a sodium-channel blocker aimed to inhibit action potential) insensitive release of transmitters from non-tanycyte cell types of the ME, an outside-out patch clamp experiment was performed. Glutamate treatment caused large inward currents (−181.29 ± 28.43 pA, n = 4, $p < 0.01$) (Figure 3B) even when the tanycyte cell body was displaced into the third ventricle. The effect of glutamate disappeared during the washout period, indicating that the observed effect of glutamate was exerted directly on the β2-tanycytes.

In contrast to glutamate, TRH had no effect on the membrane potential of tanycytes even in a relatively high concentration (1μM; N = 12; Figure S2).

Functional AMPA, Kainate, and GRM4 Receptors Are Present on β2-Tanycytes in Mice

To investigate the receptor types that mediate glutamate-induced depolarization of β2-tanycytes, the effects of glutamate receptor agonists were studied. Similar to glutamate, both AMPA (100 μM;

Expression in Beta Tanycytes (CTgeomean $_{housekeeping\ genes}$ - Ctgene ± SEM)	Short Name of the Gene	Description
Genes Expressed in Tanycytes		
5.52 ± 0.92	SLC1A1	Solute carrier family 1, member 1
4.50 ± 0.34	SLC1A2	Solute carrier family 1, member 2
−0.15 ± 0.26	SLC1A3	Solute carrier family 1, member 3
2.89 ± 0.17	GRIA1	Glutamate receptor, ionotropic, AMPA1 (alpha 1)
4.37 ± 0.51	GRIA2	Glutamate receptor, ionotropic, AMPA2 (alpha 2)
5.97 ± 0.68	GRIK2	Glutamate receptor, ionotropic, kainate 2 (beta 2)
−0.59 ± 0.10	GRIK3	Glutamate receptor, ionotropic, kainate 3
5.81 ± 0.27	GRIK4	Glutamate receptor, ionotropic, kainate 4
2.57 ± 0.35	GRIK5	Glutamate receptor, ionotropic, kainate 5 (gamma 2)
3.15 ± 0.09	GRIN3A	Glutamate receptor ionotropic, NMDA3A
5.29 ± 0.16	GRM4	Glutamate receptor, metabotropic 4
1.57 ± 0.25	DIO2	Deiodinase, iodothyronine, type II
5.46 ± 0.31	DAGLA	Diacylglycerol lipase, alpha
Genes Not Expressed in Tanycytes		
8.07 ± 0.61	SLC1A6	Solute carrier family 1, member 6
UD	SLC1A7	Solute carrier family 1, member 7
6.83 ± 1.68	GRIA3	Glutamate receptor, ionotropic, AMPA3 (alpha 3)
6.85 ± 0.58	GRIA4	Glutamate receptor, ionotropic, AMPA4 (alpha 4)
10.24 ± 0.33	GRIK1	Glutamate receptor, ionotropic, kainate 1
6.80 ± 0.75	GRIN1	Glutamate receptor, ionotropic, NMDA1 (zeta 1)
6.88 ± 0.30	GRIN2A	Glutamate receptor, ionotropic, NMDA2A (epsilon 1)
6.54 ± 0.21	GRIN2B	Glutamate receptor, ionotropic, NMDA2B (epsilon 2)
UD	GRIN2C	Glutamate receptor, ionotropic, NMDA2C (epsilon 3)
8.26 ± 0.62	GRIN2D	Glutamate receptor, ionotropic, NMDA2D (epsilon 4)
UD	GRIN3B	Glutamate receptor, ionotropic, NMDA3B
11.77 ± 1.98	GRM1	Glutamate receptor, metabotropic 1
UD	GRM2	Glutamate receptor, metabotropic 2
6.88 ± 1.21	GRM3	Glutamate receptor, metabotropic 3
6.38 ± 0.73	GRM5	Glutamate receptor, metabotropic 5
UD	GRM6	Glutamate receptor, metabotropic 6
9.20 ± 0.27	GRM7	Glutamate receptor, metabotropic 7

Table 1. Expression of Glutamate Receptors and Transporters in β-Tanycytes

(Continued on next page)

Expression in Beta Tanycytes (CTgeomean $_{housekeeping\ genes}$ - Ctgene ± SEM)	Short Name of the Gene	Description
UD	GRM8	Glutamate receptor, metabotropic 8
8.08 ± 0.41	TRHR1	Thyrotropin-releasing hormone receptor 1
6.86 ± 1.59	TRHR2	Thyrotropin-releasing hormone receptor 2

Table 1. Continued

Genes were considered to be expressed in β-tanycytes if the ΔCT value was lower than the ΔCT of GRM5. See also Figure S4 and Table S1.

5.37 ± 1.09 mV; n = 8, p < 0.001; Figure 3C) and kainate (125 μM; 8.04 ± 2.08 mV, n = 7, p < 0.001; Figure 3D) markedly depolarized the β-tanycytes. Bath application of the AMPA and kainate receptor antagonist, DNQX (500 μM), prevented these effects (Figures 3C and 3D).

In contrast to AMPA and kainate, NMDA had no effect on the membrane potential of tanycytes, even at high concentration (0.5 mM: 1.41 ± 0.65 mV, n = 3, p = 0.42 and 4 mM: 2.12 ± 0.3 mV, n = 3, p = 1.00. Figure S3). Administration of the GRM4 agonist VU 0155041 caused a small, but significant, hyperpolarization (1 mM; −1.48 ± 0.54 mV, n = 10, p < 0.01) of the membrane potential of β2-tanycytes (Figure S3F) indicating that it is unlikely that activation of GRM4 contributes to the glutamate-induced depolarization of tanycytes.

Glutamate Depolarized the β2-Tanycytes via Both AMPA and Kainate Receptors and Also by TBOA-Sensitive Glutamate Transport in Mice

To determine whether the effect of glutamate on the membrane potential of β2-tanycytes is mediated exclusively via AMPA and kainate receptors, hypothalamic slices were treated with glutamate in the presence of DNQX. Inhibition of the kainate and AMPA receptors caused a significant but only partial inhibition of the β2-tanycytes (glutamate: 9.18 ± 1.55 mV, n = 9, p < 0.001 versus control; glutamate + DNQX: 5.23 ± 1.24 mV, p < 0.001 versus control and p = 0.019 versus glutamate; Figure 3F). Therefore, we determined whether glutamate transport also contributes to the glutamate-induced depolarization. Similar to DNQX, the glutamate transporter inhibitor TBOA caused a partial inhibition of the glutamate-induced depolarization (glutamate + TBOA: 4.68 ± 0.91 mV, n = 9, p = 0.001 versus control and p = 0.002 vs. glutamate; Figure 3E). However, the combination of DNQX and TBOA completely blocked the effect of glutamate (0.40 ± 0.61 mV, n = 9, p = 1.00 versus control and p < 0.001 vs. glutamate; Figure 3E), demonstrating that glutamate depolarizes the tanycytes via a combination of AMPA and kainate receptor-mediated effects and glutamate transport.

The Effect of TRH Axon Activation on Tanycytes Is Mediated Partially by Glutamate in Mice

Optogenetic activation of the axon terminals of the TRH neurons around the endfeet processes of β2-tanycytes in the external zone of the median eminence consequently caused a 0.75 ± 0.14 mV (p < 0.001) depolarization of the patched β2-tanycyte cell bodies in the ventricular wall of the ME (Figure 4). The peak of the depolarization was reached 51.74 ± 2.93 ms after the start of the optogenetic activation; the velocity of this depolarization was 0.016 ± 0.005 mV/ms. Examination of the first derivative (dV/dt) of the membrane potential showed two peaks, suggesting that the repolarization has two phases (Figure 4C). The fast depolarization was followed by a fast −0.29 ± 0.09 mV repolarization with 126.66 ± 10.73 ms decay time and then by a very slow repolarization (decay time: 3,127.60 ± 446.29 ms). This suggested that the TRH axons may influence tanycytes by the release of at least two different compounds: a fast-acting transmitter and a transmitter with long-lasting effect. Simultaneous administration of DNQX and TBOA markedly decreased the optogenetic activation-induced depolarization of tanycytes (0.32 ± 0.08 mV; p < 0.01; Figure 4). The velocity of this depolarization was significantly lower than the velocity of depolarization induced by glutamate alone (0.004 ± 0.002; p < 0.05; Figure 4E). The first derivative (dV/dt) of the membrane potential had only one peak (Figure 4C) in the presence of antagonists, indicating that this effect has only one phase. The two antagonists prevented the first fast phase. These data demonstrate that the TRH axons influence the tanycytes with a fast-acting transmitter, glutamate, and also by a currently unknown transmitter(s) with longer-lasting effect.

Optic stimulation of slices from TRH-IRES-tdTomto mice where the TRH axons expressed tdTomato (but did not express channelrhodopsin) had no effect on the membrane potential of tanycytes (Figure 4B).

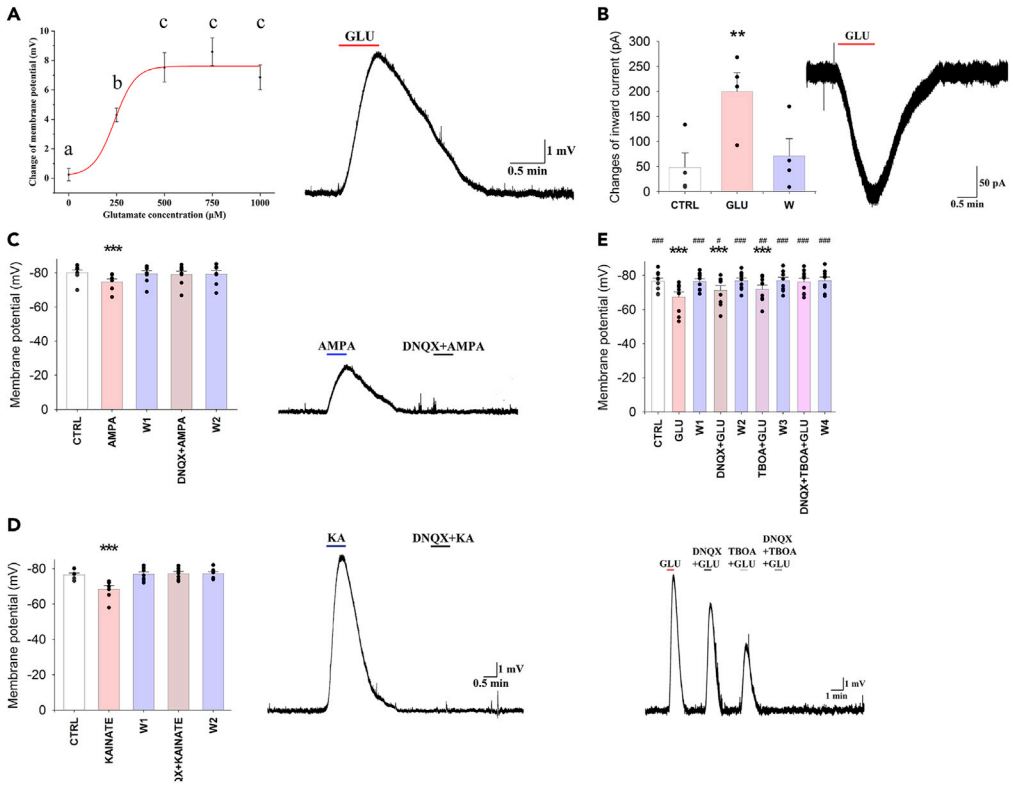

Figure 3. Glutamate Depolarizes the β2-Tanycytes via Activation of AMPA and Kainate Receptors and via Glutamate Transport

Representative traces illustrate the effects of pharmacological treatments on the β2-tanycytes.

(A) Glutamate induced a dose-dependent depolarization of β2-tanycytes ($N_{Control}$ = 6; $N_{250\mu M}$ = 11; $N_{500\mu M}$ = 12; $N_{750\mu M}$ = 8; $N_{1000\mu M}$ = 6). A representative trace illustrates the change of the membrane potential of a β2-tanycyte in response to 500 μM glutamate.

(B–D) (B) Glutamate (500 μM; N = 4) evoked a large inward current on β2-tanycyte outside-out preparations, demonstrating that glutamate directly influences the tanycytes. Similar to glutamate, both (C) AMPA (100 μM; N = 8) and (D) kainate (125 μM; N = 7) depolarized the β2-tanycytes, and the effects prevented by the administration of the AMPA and kainate receptor antagonist, DNQX (500 μM).

(E) Although DNQX (500 μM; N = 9) and TBOA (1 mM; N = 9) caused significant, but only partial, reduction of the glutamate-induced depolarization, the combination of the two inhibitors completely blocked the effect of glutamate (N = 9), indicating that the effect of glutamate on the membrane potential of β2-tanycytes is mediated via AMPA and kainate receptors and by TBOA-sensitive glutamate transport. Data are expressed as mean ± SEM and were analyzed with repeated measure ANOVA followed by Bonferroni post hoc test.

Data with different letters on (A) are significantly different ($p < 0.05$). * significantly different from control; # significantly different from glutamate treatment. #$p < 0.05$; ** and ##$p < 0.01$; *** and ###$p < 0.001$. Abbreviations: CTRL, control; GLU, glutamate; KA, kainate;W, washout. See also Figures S2 and S3.

Effect of Glutamate and TRH on the Intracellular Ca^{2+} Levels of Tanycytes in Mice

As increase of intracellular Ca^{2+} levels is a crucial signal to increase DAGlα activity (Piomelli, 2003), the effect of glutamate was studied on the intracellular Ca^{2+} level of β2-tanycytes. Glutamate treatment (500 μM) caused a robust increase of fluorescent intensity values (FIV) of β2-tanycytes (baseline: 189.19 ± 26.52 treatment: 416.13 ± 31.28; $p < 0.001$; N_{cell} = 56) increasing it to 219.95 ± 27.66% of the baseline values (Figure 5). To determine whether similar to the effect of glutamate on the membrane potential of tanycytes, the effect of glutamate on the intracellular Ca^{2+} level can also be blocked by inhibition of AMPA and kainite receptors and glutamate transport, we administered DNQX (0.5 mM) and TBOA (1 mM) during the glutamate treatment. Application of these inhibitors completely prevented the increase of FIV (baseline: 242.13 ± 28.06 treatment: 250.27 ± 28.67; Ncell = 79; p = 0.99) (Figure 5).

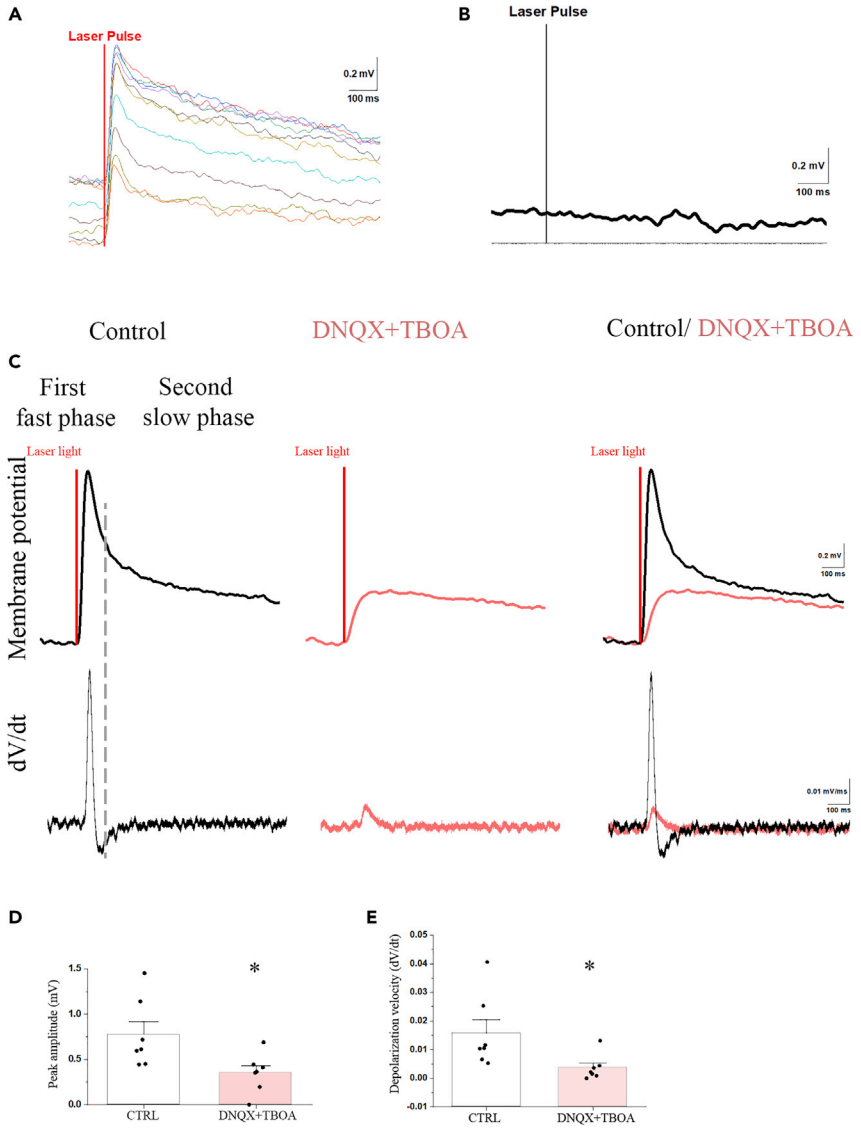

Figure 4. The Optogenetic Activation of TRH Axons in the ME Induces Depolarization of β2-Tanyctes Which Effect Is Partially Mediated by Glutamate

(A and B) The membrane potential changes of a representative tanycyte in response to 10 consecutive optic activation of TRH axons (A). The membrane potential of tanycytes is not influenced by the light impulse if the TRH axons do not express channelrhodopsin (B).

(C-E) (C) The mean response of the tanycyte membrane potential in response to 10 sweeps of optic stimulation of TRH axons. The upper traces show the membrane potential changes of the tanycyte under control conditions (black line), when the same cell was treated with a combination of DNQX (0.5 μM) and TBOA (1 mM) (red) and the overlay of the two traces. The lower graphs illustrate the first derivative (dV/dt) of the membrane potential changes. The two peaks of the dV/dt of the control trace suggest that the optic stimulation-induced membrane potential change has two phases under control conditions: an initial fast phase including a fast depolarization and a fast repolarization followed by a long-lasting phase of slow repolarization. When inhibitors are applied, the membrane potential change has only a single phase and markedly decreased amplitude. The overlay of the two traces indicates that the speed of depolarization is markedly decreased in the presence of DNQX and TBOA. Bar graphs summarize the effects of activation of TRH axons on the peak amplitude of membrane potential (D) and the depolarization velocity (E) under control condition and when the cells are treated with DNQX + TBOA.

Data are expressed as mean ± SEM and were analyzed with paired Student's t test. * significantly different ($p < 0.05$).

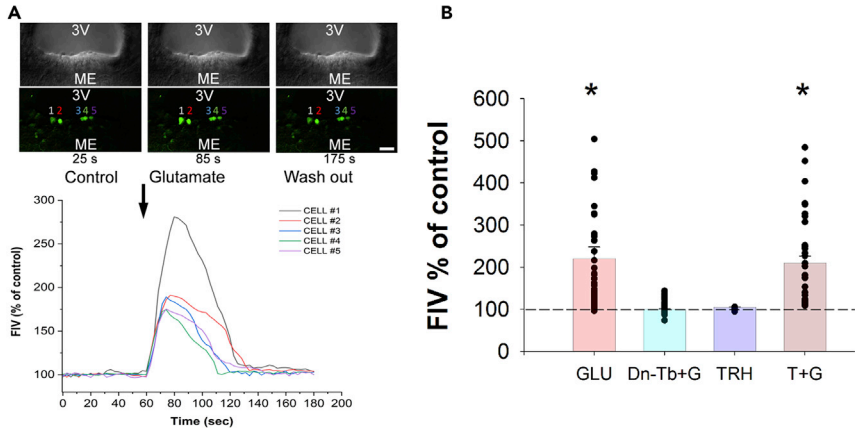

Figure 5. Effects of Glutamate and TRH Treatment on the Intracellular Ca^{2+} Level of β2-Tanycytes

The changes of fluorescent intensity values (FIV) of the Ca^{2+}-sensitive dye Fluo-4 AM was measured as a marker of the changes of intracellular Ca^{2+} level of β2-tanycytes after different treatments *in vitro*.

(A) Representative recording shows that glutamate treatment (500 μM) increases FIVs in the measured β2-tanycyte perikarya. Black arrow represents the beginning of the glutamate treatment.

(B) Bar graph summarizes effects of different treatments. GLU, glutamate (500 μM, N = 56); Dn-Tb + G, DNQX + TBOA + GLU (DNQX + TBOA, 0.5 mM and 1 mM, respectively; N = 79); TRH (5 μM, N = 34); T + G, TRH + glutamate (5 and 500 μM, respectively; N = 37). Only glutamate and TRH + glutamate treatment increased FIV% values significantly ($p < 0.001$ and $p = 0.002$, respectively). TRH alone could not initiate any significant changes. The effects of Glutamate alone and the combined Glutamate + TRH treatment did not differ from each other ($p = 0.999$). Treatment of sections with DNQX + TBOA prevented the increase of intracellular Ca^{2+} level induced by glutamate treatment (DNQX + TBOA + GLU versus control: $p = 0.999$). Data are shown as mean ± SEM, for statistical comparison one-way ANOVA ($F(4, 235) = 15.849$; $p < 0.0001$) was used followed by Bonferroni post hoc test. * significantly different from control $p < 0.05$. Scale bar, 50 μm.

To test whether the main transmitter of the hypophysiotropic TRH neurons can influence the intracellular Ca^{2+} level of β2 tanycytes, the effects of TRH and its combination with glutamate were tested (Figure 5). TRH treatment (5 μM) caused no significant changes either in the FIV of β2-tanycytes (control: 187.46 ± 30.58 treatment: 186.71 ± 30.42) or in the percentage values of FIV (99.79 ± 0.30%) when compared with the control, baseline values ($p = 0.9$; $N_{cell} = 34$).

Treatment of β2-tanycytes with the combination of TRH + Glutamate (5 and 500 μM, respectively) caused a robust increase of FIV (control: 154.70 ± 26.09, treatment: 323.85 ± 34.68) increasing it to 209.34 ± 16.88% of the baseline values ($p = 0.002$; $N_{cell} = 37$). The effect of combined TRH + glutamate treatment, however, did not differ from the effect of treatment with glutamate alone ($p = 0.99$).

A positive allosteric modulator of GRM4 receptor VU0155041 (1.5 mM) caused no significant changes either in the FIV of β2-tanycytes (control: 76.01 ± 16.56, treatment: 77.13 ± 16.43) or the percentage values (102.90 ± 1.39%) when compared with the control, baseline values ($p = 0.9$; $N_{cell} = 21$).

Effect of the Inhibition of Glutamate Action on the 2-AG Content of the Rat Median Eminence Explants

To determine whether endogenous glutamate can stimulate the 2-AG synthesis of tanycytes, the effect of glutamate receptor and transporter inhibitors was studied on the 2-AG content of ME explants. The 2-AG content of control ME explants was readily detected (0.54 ± 0.08 ng/mg tissue). Simultaneous inhibition of AMPA and kainate receptors and the TBOA-sensitive glutamate transporters caused an approximately 50% decrease of the 2-AG content of the ME explants (0.29 ± 0.03 ng/mg tissue; $p = 0.01$) suggesting that endogenous glutamate stimulates 2-AG synthesis in tanycytes.

DISCUSSION

Endocannabinoids are well known as retrograde transmitters used by neurons to control their own neuronal inputs (Mayer et al., 1984; Ohno-Shosaku and Kano, 2014). In the current manuscript, however,

we demonstrate that the β-tanycytes of the ME also utilize endocannabinoids to regulate TRH release from hypophysiotropic neurons.

To establish the importance of the endocannabinoid system in regulating hypophysiotropic TRH neurons, we demonstrated that the majority of TRH neurons in the PVN expresses CB1 mRNA and that CB1 protein is present on the axon varicosities of the hypophysiotropic TRH neurons that terminate around the portal capillaries in the external zone of the ME. This observation is especially intriguing as only very few neuronal perikarya are present in the ME and the majority are located in the subependymal zone (Rethelyi, 1975). Thus, neurons are virtually absent from the external zone of the ME. As endocannabinoids can travel only extremely short distances in the neuropil before degradation (Regehr et al., 2009), the lack of neurons in the external zone of the ME excludes a neuronal origin of endocannabinoids to act on CB1 on hypophysiotropic axon terminals.

The main endocannabinoid that acts on CB1 is 2-AG (Tanimura et al., 2010) and synthesized by DAGLα (Tanimura et al., 2010). DAGLα-immunoreactivity was observed in cell bodies and basal processes of β-tanycytes in the ME. Immunoelectron microscopy further established the presence of DAGLα in β-tanycytes and demonstrated its location not only in tanycyte cell bodies, but also in their basal processes with high concentrations in the endfeet processes around portal capillaries. This is in contrast to the data of Suarez et al. (2010), who observed DAGLα immunoreactivity only in the apical part of tanycyte cell bodies. To determine whether the reason of this discrepancy may be species difference, DAGLα immunostaining was performed in the ME of rats. Similar to the observation of Suarez et al. (2010), we observed strong DAGLα immunoreactivity in the cell bodies of tanycytes in the ME, and we also observed DAGLα immunoreactivity in the basal processes of tanycytes, indicating that DAGLα is present in tanycyte processes in both species. The absence of DAGLα immunoreactivity in the ME of DAGLα knockout (KO) mice clearly demonstrates the specificity of our findings. We observed CB1-IR varicosities closely associated to DAGLα-IR tanycyte processes in the external zone of the ME and, specifically, CB1-IR TRH varicosities in juxtaposition to DAGLα-IR tanycyte processes. Thus, tanycytes are in position to regulate TRH release from hypophysiotropic axon terminals in the ME.

In agreement with the morphological findings, the CB1 antagonist, AM251, increased the amount of TRH released from ME explants indicating a tonic inhibitory effect of endocannabinoids on the release of TRH. Surprisingly, incubation with the CB1 agonist WIN55,212-2 had no effect on TRH release from ME explants. However, when endocannabinoid synthesis was inhibited by THL, TRH release from the explants increased and this was prevented by WIN55,212-2. We presume that tanycytes may tonically release high concentrations of endocannabinoids in ME explants that are sufficient to saturate CB1 receptors in hypophysiotropic TRH terminals; therefore, a further increase in agonist activity by WIN55,212-2 would not be expected to influence TRH release. This hypothesis is supported by the observation that, when the synthesis of endocannabinoids is blocked in the ME explants, the lower occupancy of CB1 receptors permits CB1 agonist-induced inhibition of TRH release, further demonstrating the key and dynamic role of tanycytes in the regulation of the HPT axis.

In contrast to the inhibitory effect of endocannabinoids on the TRH release, PGE2 has been shown to cause retraction of tanycyte processes allowing access of hypophysiotropic axons to capillaries, thus facilitating hormone release (de Seranno et al., 2010). Intriguingly, the synthesizing enzymes of PGE2, cyclooxygenase (COX)-1 and COX-2, are synthesized in tanycytes (de Seranno et al., 2010), and arachidonic acid (AA) is similarly necessary for the synthesis of endocannabinoids and PGE2 (Malcher-Lopes and Buzzi, 2009). In the immune system, humoral signals can shift the balance between the endocannabinoid and prostaglandin system that plays, for example important role in the mediation of the effects of glucocorticoids (Malcher-Lopes and Buzzi, 2009). Thus, it is feasible to hypothesize that humoral signals may also regulate the balance of these two antagonistic signaling systems in the tanycytes to cause simultaneous regulation of hormone release and capillary access of hypophysiotropic terminals. However, this hypothesis requires further studies.

In neuronal circuits, glutamate is an important driving force of endocannabinoid synthesis (Piomelli, 2003). Presynaptically released glutamate binds to Grm1 and Grm5, and the activation of these metabotropic glutamate receptors stimulate the DAGLα via an increase in intracellular Ca^{2+} levels (Katona et al., 2006; Piomelli, 2003). In the external zone of the ME, there are no synapses between TRH axons and tanycyte processes, but glutamate that is released from the hypophysiotropic TRH axons (Hrabovszky et al., 2005) into the extracellular space is well positioned to influence tanycytes due to the close juxtaposition of the two cells. Our *in situ* hybridization data indicated that Grm1 and Grm5 are not present in tanycytes, but

kainate and AMPA receptor subunits have been previously described in β-tanycytes (Kawakami, 2000; Eyigor and Jennes, 1998). In agreement with these findings, we detected the GRIA1 and GRIA2 AMPA receptor subunits and the GRIK3 kainate receptor subunit as the glutamate receptor subunits expressed in β-tanycytes. The GRIK2, GRIK4, and GRIK5 kainate receptor subunits and mGLU4 are also expressed, but at a much lower level. In contrast, expression of NMDA and the other metabotropic glutamate receptor subunits was barely detectable.

The presence of glutamate receptor subunits in β-tanycytes strongly suggested that glutamate influences β-tanycytes. Indeed, patch clamp electrophysiology experiments showed that the administration of glutamate dose-dependently depolarizes β-tanycytes. Similarly, kainate and AMPA also depolarized β-tanycytes, suggesting the importance of AMPA and/or kainate receptors in the mediation of the glutamate-induced regulation of tanycytes. Inhibition of these receptors, however, only partially inhibited glutamate-induced depolarization. Administration of GRM4 agonist caused a small hyperpolarization of β-tanycytes excluding the possibility that this receptor could be involved in the mediation of glutamate-induced depolarization of tanycytes. Since in addition to the receptor-mediated effect, glutamate also causes depolarization by uptake of glutamate via specific glutamate transporters (Kim et al., 2008), we tested the presence of glutamate transporters in β-tanycytes. A high level of expression of the glutamate transporter SLC1A3 was observed in β-tanycytes. Accordingly, simultaneous inhibition of AMPA and kainate receptors and glutamate transporters completely blocked the glutamate-induced depolarization of β-tanycytes. Thus, the two ionotropic glutamate receptor types as well as the glutamate transporter are critical for the glutamate-induced regulation of this cell type.

To determine whether hypophysiotropic TRH axons can influence the β-tanycytes by glutamate release, an optogenetic experiment was performed. Using combined optogenetic activation of the hypophysiotropic TRH axons and the patch clamp recording of β2-tanycyte cell bodies, we showed that TRH axon activation causes a biphasic depolarization of tanycytes. The fast component of this depolarization can be prevented by administration of DNQX and TBOA demonstrating that the fast component of this depolarization is caused by glutamate release of the TRH axons. The slower and more prolonged component of the tanycyte depolarization was not influenced by glutamate inhibitors suggesting that the TRH axons also use other transmitters to influence tanycytes.

As peptides could have longer-lasting effect compared with glutamate and the work by Muller-Fielitz et al. (2017) showed that TRH increases the intracellular Ca^{2+} level of β-tanycytes via TRHR1, we hypothesized that this long-lasting effect could be due to the TRH release of hypophysiotropic axons. Owing to the lack of TRH antagonists, we tested the effect of TRH on the membrane potential of tanycytes. Administration of a relatively high TRH dose (1 μM), however, had no effect on the membrane potential of tanycytes. TRH also did not have effect on the intracellular Ca^{2+} level of tanycytes, and we could not detect expression of any TRH receptor in the transcriptome of tanycytes isolated by laser capture microdissection. Explanation for the discrepancy between these two observations is uncertain, but we note that Muller-Fielitz et al. (2017) used an extremely high, pharmacological dose of TRH (30 μM) in their studies. Our data, however, exclude the possibility that activation of TRH axons causes the long-lasting depolarization of tanycytes via release of TRH. Further studies are needed to determine the mechanism of this effect.

The activation of TRH axons resulted in less depolarization of tanycytes than the administration of glutamate. We have to consider, however, that exogenous glutamate can act on the entire surface of tanycytes including their cell body, whereas transmitters released from the TRH axons can act only on the endfeet processes of tanycytes that are located far, approximately 80–100 μm, from the tanycyte cell bodies where the membrane potential was measured.

How depolarization regulates glial endocannabinoid synthesis is yet unknown, but an increase in intracellular Ca^{2+} level is a well-known activator of DAGLα (Katona et al., 2006). Using Ca^{2+} imaging, we demonstrated that glutamate not only depolarizes β-tanycytes, but also increases the intracellular Ca^{2+} level of these cells. This effect of glutamate was also blocked by inhibition of the AMPA and kainite receptors and glutamate transport indicating that glutamate influences the membrane potential and the intracellular Ca^{2+} level of tanycytes via similar mechanisms. The effect of glutamate on the intracellular Ca^{2+} level of tanycytes suggests that glutamate can stimulate the endocannabinoid synthesis of tanycytes. Indeed, inhibition of the AMPA and kainite receptors together with inhibition of glutamate transport markedly

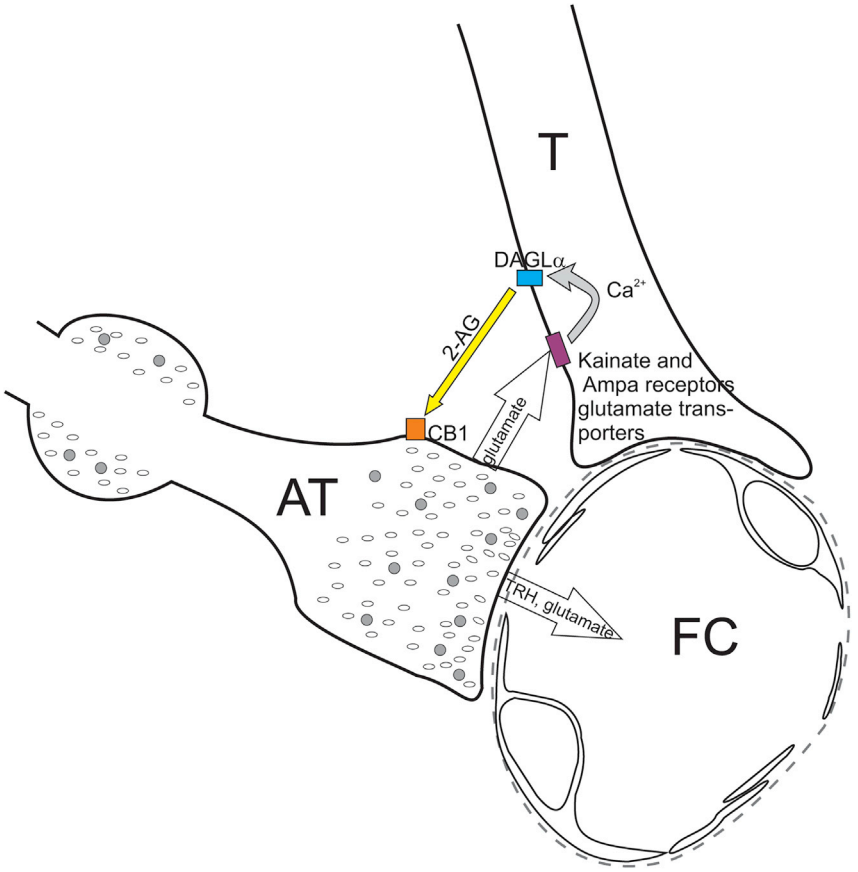

Figure 6. Schematic Illustration of the Neuro-glial Microcircuit in the External Zone of the ME

Axon terminals (AT) of the hypophysiotropic TRH neurons are closely associated to the endfeet processes of tanycytes (T) in the vicinity of fenestrated capillaries (FC) of the hypophyseal portal circulation. The TRH axons release glutamate that stimulates the DAGLα activity of tanycytes, and therefore the 2-AG synthesis of these cells, by acting through kainite and AMPA receptors and glutamate transport and by the resulting increase of intracellular Ca^{2+} level. The released endocannabinoids bind to the CB1 of the hypophysiotropic TRH axons and inhibit the amount of TRH released into the portal capillary.

decreased the 2-AG content of the ME explants demonstrating that endogenous glutamate has a stimulatory effect on the 2-AG synthesis in the ME.

Regulation of TRH release by this novel neuroglial microcircuit utilizing endocannabinoids and glutamate may be important for regulating pulsatile TRH release by synchronizing the activity of hypophysiotropic axon terminals. However, in addition to the TRH-containing CB1-IR terminals, CB1 immunoreactivity is also present in the external zone of the ME in hypophysiotropic terminals other than the axons of hypophysiotropic TRH neurons, suggesting that regulation of hypophysiotropic terminals by tanycyte-derived endocannabinoids may play a more generalized role in the control of the neuroendocrine systems.

In summary, these data demonstrate that a regulatory microcircuit exists between β-tanycytes and hypophysiotropic TRH axons, utilizing the release of endocannabinoids and glutamate (Figure 6). This circuit may contribute to controlling the release of TRH into the ME and may be an important mechanism to synchronize the activity of hypophysiotropic terminals.

Limitations of the Study

Although the morphological and electrophysiological experiments were done in mice, the explant experiments had to be performed in a different species, in rats, because of the very small volume of the mouse median eminence.

METHODS

All methods can be found in the accompanying Transparent Methods supplemental file.

SUPPLEMENTAL INFORMATION

Supplemental Information can be found online at https://doi.org/10.1016/j.isci.2020.100921.

ACKNOWLEDGMENT

This work was supported by Grants from the Hungarian Science Foundation (OTKA K109710), the Hungarian National Brain Research Program (2017-1.2.1-NKP-2017-00002), EU H2020 THYRAGE no. 666869, CONACYT-Mexico (CB2015/254960), ERC682426, KFI-2016-0177, GINOP-2016-00979, NVKP-2016-0043 and by the BME-Biotechnology FIKP grant of EMMI (BME FIKP-BIO). The authors express their gratitude to Zsófia László for her help during the preparing of some of the confocal microscopic images.

AUTHOR CONTRIBUTIONS

E.F. performed the immunofluorescent and ultrastructural studies. E.V. and B.K. designed and performed the patch clamp experiments. B.K. performed the optogenetic experiments. Z.P. deigned and performed the calcium imaging experiments. A.C.-V., J.-L.C., P.J.-B., A.S.-S., and Y.R. designed and performed the ME explant experiments and analyzed these data. M.M. synthesized, purified, and chemically characterized P-TRH. B.T. performed the 2-AG measurement. M.T. performed and analyzed the *in situ* hybridization experiments. F.E., Z.M., G. S., and B.G. were involved in the generation of TRH-IRES-Cre mice. A.S.-S. and D.K. isolated the tanycytes and performed the gene expression analysis. D.Z. performed the stereotaxic AAV injections. A.K. performed immunostaining. Zs.M. and B.R. helped to design and perform the calcium imaging experiments and analyzed data. M.W. provided CB1 antibody. M.K. provided tissues of DAGLα KO mice. K.M. provided DAGLα antibody. R.M.L. analyzed data and wrote the manuscript. C.F. acquired the funding, conceptualized and interpreted the studies, and wrote the manuscript.

DECLARATION OF INTERESTS

B.R. is one of the founders of Femtonics and is a member of its scientific advisory board. The other authors have declared that no conflict of interest exists.

Received: March 25, 2019
Revised: May 20, 2019
Accepted: February 12, 2020
Published: March 27, 2020

REFERENCES

de Seranno, S., D'anglemont De Tassigny, X., Estrella, C., Loyens, A., Kasparov, S., Leroy, D., Ojeda, S.R., Beauvillain, J.C., and Prevot, V. (2010). Role of estradiol in the dynamic control of tanycyte plasticity mediated by vascular endothelial cells in the median eminence. Endocrinology *151*, 1760–1772.

Eyigor, O., and Jennes, L. (1998). Identification of kainate-preferring glutamate receptor subunit GluR7 mRNA and protein in the rat median eminence. Brain Res. *814*, 231–235.

Fekete, C., and Lechan, R.M. (2014). Central regulation of hypothalamic-pituitary-thyroid axis under physiological and pathophysiological conditions. Endocr. Rev. *35*, 159–194.

Fekete, C., Sarkar, S., Christoffolete, M.A., Emerson, C.H., Bianco, A.C., and Lechan, R.M. (2005). Bacterial lipopolysaccharide (LPS)-induced type 2 iodothyronine deiodinase (D2) activation in the mediobasal hypothalamus (MBH) is independent of the LPS-induced fall in serum thyroid hormone levels. Brain Res. *1056*, 97–99.

Freitas, B.C., Gereben, B., Castillo, M., Kallo, I., Zeold, A., Egri, P., Liposits, Z., Zavacki, A.M., Maciel, R.M., Jo, S., et al. (2010). Paracrine signaling by glial cell-derived triiodothyronine activates neuronal gene expression in the rodent brain and human cells. J. Clin. Invest. *120*, 2206–2217.

Hrabovszky, E., Wittmann, G., Turi, G.F., Liposits, Z., and Fekete, C. (2005). Hypophysiotropic thyrotropin-releasing hormone and corticotropin-releasing hormone neurons of the rat contain vesicular glutamate transporter-2. Endocrinology *146*, 341–347.

Kano, M., Ohno-Shosaku, T., Hashimotodani, Y., Uchigashima, M., and Watanabe, M. (2009). Endocannabinoid-mediated control of synaptic transmission. Physiol. Rev. *89*, 309–380.

Katona, I., Urban, G.M., Wallace, M., Ledent, C., Jung, K.M., Piomelli, D., Mackie, K., and Freund, T.F. (2006). Molecular composition of the endocannabinoid system at glutamatergic synapses. J. Neurosci. *26*, 5628–5637.

Kawakami, S. (2000). Glial and neuronal localization of ionotropic glutamate receptor subunit-immunoreactivities in the median eminence of female rats: GluR2/3 and GluR6/7 colocalize with vimentin, not with glial fibrillary acidic protein (GFAP). Brain Res. *858*, 198–204.

Kim, M.H., Uehara, S., Muroyama, A., Hille, B., Moriyama, Y., and Koh, D.S. (2008). Glutamate transporter-mediated glutamate secretion in the mammalian pineal gland. J. Neurosci. *28*, 10852–10863.

Lechan, R.M., and Fekete, C. (2007). Infundibular tanycytes as modulators of neuroendocrine function: hypothetical role in the regulation of the thyroid and gonadal axis. Acta Biomed. *78* (*Suppl 1*), 84–98.

Malcher-Lopes, R., and Buzzi, M. (2009). Glucocorticoid-regulated crosstalk between arachidonic acid and endocannabinoid biochemical pathways coordinates cognitive-, neuroimmune-, and energy homeostasis-related adaptations to stress. Vitam Horm. *81*, 263–313.

Mayer, M.L., Westbrook, G.L., and Guthrie, P.B. (1984). Voltage-dependent block by Mg2+ of NMDA responses in spinal cord neurones. Nature *309*, 261–263.

Muller-Fielitz, H., Stahr, M., Bernau, M., Richter, M., Abele, S., Krajka, V., Benzin, A., Wenzel, J., Kalies, K., Mittag, J., et al. (2017). Tanycytes control the hormonal output of the hypothalamic-pituitary-thyroid axis. Nat. Commun. *8*, 484.

Ohno-Shosaku, T., and Kano, M. (2014). Endocannabinoid-mediated retrograde modulation of synaptic transmission. Curr. Opin. Neurobiol. *29*, 1–8.

Pak, T., Yoo, S., Miranda-Angulo, A.L., Wang, H., and Blackshaw, S. (2014). Rax-CreERT2 knock-in mice: a tool for selective and conditional gene deletion in progenitor cells and radial glia of the retina and hypothalamus. PLoS One *9*, e90381.

Piomelli, D. (2003). The molecular logic of endocannabinoid signalling. Nat. Rev. Neurosci. *4*, 873–884.

Prevot, V., Dehouck, B., Sharif, A., Ciofi, P., Giacobini, P., and Clasadonte, J. (2018). The versatile tanycyte: a hypothalamic integrator of reproduction and energy metabolism. Endocr. Rev. *39*, 333–368.

Regehr, W.G., Carey, M.R., and Best, A.R. (2009). Activity-dependent regulation of synapses by retrograde messengers. Neuron *63*, 154–170.

Rethelyi, M. (1975). Neurons in the subependymal layer of the rat median eminence. Neuroendocrinology *17*, 330–339.

Rodriguez-Rodriguez, A., Lazcano, I., Sanchez-Jaramillo, E., Uribe, R.M., Jaimes-Hoy, L., Joseph-Bravo, P., and Charli, J.L. (2019). Tanycytes and the control of thyrotropin-releasing hormone flux into portal capillaries. Front. Endocrinol. (Lausanne) *10*, 401.

Rodriguez, E.M., Blazquez, J.L., Pastor, F.E., Pelaez, B., Pena, P., Peruzzo, B., and Amat, P. (2005). Hypothalamic tanycytes: a key component of brain-endocrine interaction. Int. Rev. Cytol. *247*, 89–164.

Sanchez, E., Vargas, M.A., Singru, P.S., Pascual, I., Romero, F., Fekete, C., Charli, J.L., and Lechan, R.M. (2009). Tanycyte pyroglutamyl peptidase II contributes to regulation of the hypothalamic-pituitary-thyroid axis through glial-axonal associations in the median eminence. Endocrinology *150*, 2283–2291.

Suarez, J., Romero-Zerbo, S.Y., Rivera, P., Bermudez-Silva, F.J., Perez, J., De Fonseca, F.R., and Fernandez-Llebrez, P. (2010). Endocannabinoid system in the adult rat circumventricular areas: an immunohistochemical study. J. Comp. Neurol. *518*, 3065–3085.

Tanimura, A., Yamazaki, M., Hashimotodani, Y., Uchigashima, M., Kawata, S., Abe, M., Kita, Y., Hashimoto, K., Shimizu, T., Watanabe, M., et al. (2010). The endocannabinoid 2-arachidonoylglycerol produced by diacylglycerol lipase alpha mediates retrograde suppression of synaptic transmission. Neuron *65*, 320–327.

Wittmann, G., Deli, L., Kallo, I., Hrabovszky, E., Watanabe, M., Liposits, Z., and Fekete, C. (2007). Distribution of type 1 cannabinoid receptor (CB1)-immunoreactive axons in the mouse hypothalamus. J. Comp. Neurol. *503*, 270–279.

iScience, Volume *23*

Supplemental Information

A Glial-Neuronal Circuit in the Median Eminence Regulates Thyrotropin-Releasing Hormone-Release via the Endocannabinoid System

Erzsébet Farkas, Edina Varga, Balázs Kovács, Anett Szilvásy-Szabó, Antonieta Cote-Vélez, Zoltán Péterfi, Magdalini Matziari, Mónika Tóth, Dóra Zelena, Zsolt Mezriczky, Andrea Kádár, Dóra Kővári, Masahiko Watanabe, Masanobu Kano, Ken Mackie, Balázs Rózsa, Yvette Ruska, Blanka Tóth, Zoltán Máté, Ferenc Erdélyi, Gábor Szabó, Balázs Gereben, Ronald M. Lechan, Jean-Louis Charli, Patricia Joseph-Bravo, and Csaba Fekete

Supplementary Figures

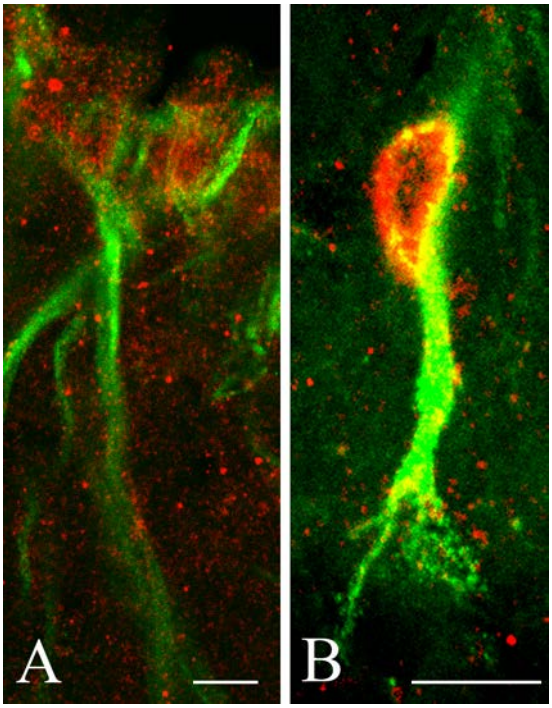

Figure S1. Expression of DAGLα in tanycytes of the rat median eminence. **Related to Figure 1.** DAGLα-immunoreactivity (red) is present in the cell bodies and basal process of vimentin-immunoreactive (green) β2- (A) and γ-tanycytes (B). γ-tanycytes are located in the external zone of the median eminence (Wittmann et al., 2017).

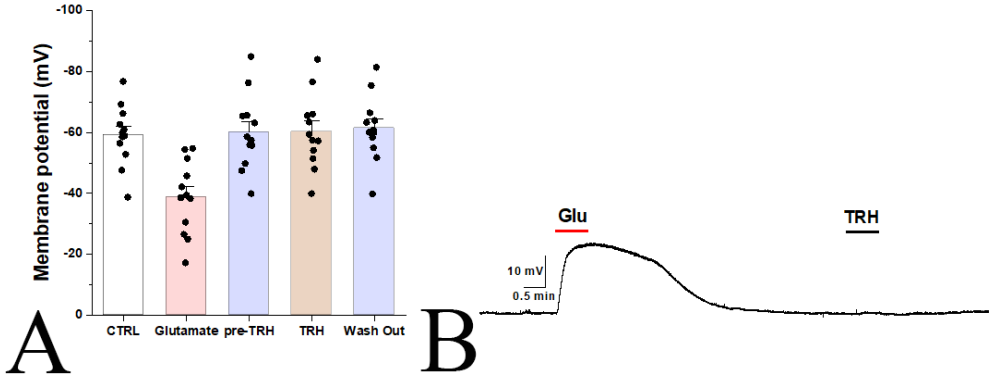

Figure S2. Effect of TRH on the membrae potential of tanycytes (N=12). **Related to Figure 3.** Bar graphs (A) show the effects of glutamate (500µM) and TRH (1µM) on the membrane potential of β2-tanycytes. While glutamate (500µM) caused a marked depolarization of tanycytes, TRH administration had no effect. A representative trace (B) illustrates the effects of glutamate and TRH on a β2-tanycyte.

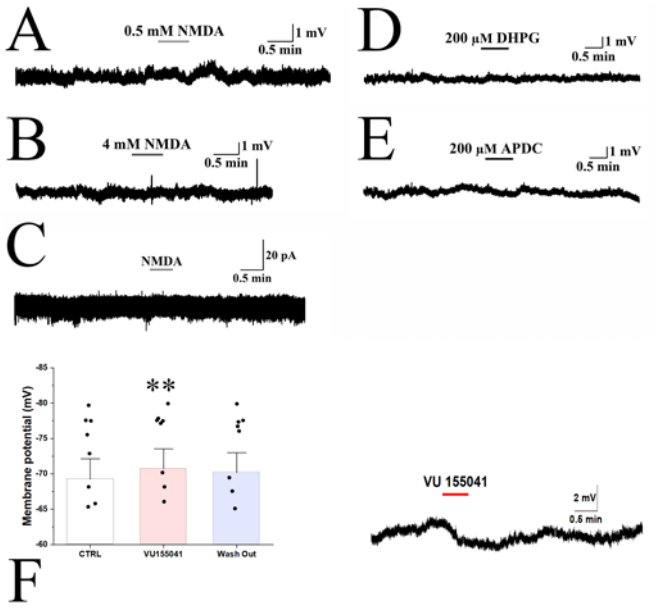

Figure S3. Effect of NMDA and metabotropic glutamate receptor agonists on the membrane potential of the β2-tanycytes. **Related to Figure 3.** Representative traces demonstrate that neither (A) 0.5 mM nor (B) 4 mM NMDA had effect on the membrane potential of β2-tanycytes. To exclude the possibility that the lack of NMDA effect is due to the magnesium block of the receptor at the resting membrane potential, the effect of NMDA was tested on β2-tanycytes held at -40 mV. (C) NMDA (0.5 mM) had also no effect on the β2-tanycytes under this condition. Neither Type I (D) nor Type II (E) metabotropic glutamate receptor agonists had an effect on the membrane potential of tanycytes. In contrast, the GRM4 agonist VU155041 (1mM) caused a small, but significant hyperpolarization of β2-tanycytes (n=10). Data are shown as mean ± SEM, for statistical comparison repeated measure ANOVA was used followed by Bonferroni post hoc test. ** = significantly different from control $P < 0.01$.

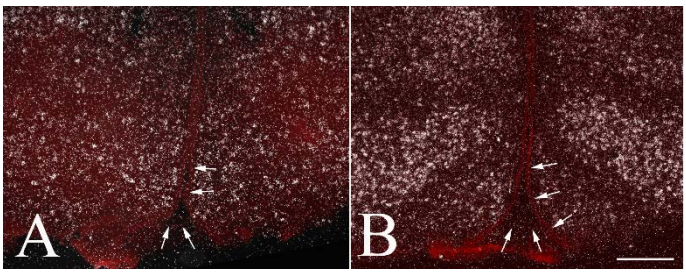

Figure S4. Distribution of *GRM1* and *GRM5* mRNA in the hypothalamus. **Related to Table 1**. Images of in situ hybridization for (A) *Grm1* and (B) GRM5 demonstrate the absence of hybridization signal (silver grains) for the tanycytes (arrows) lining the floor and lateral wall of the third ventricle. cresyl-violet counterstaining (red) labels the cell nuclei. Scale bar = 200µm

Table S1

Assay ID	Gene Symbol(s)	Gene Name(s)
18S-Hs99999901_s1	18S	18s rRNA
Mm02619580_g1	Actb	actin, beta
Mm03302249_g1	Gapdh	glyceraldehyde-3-phosphate dehydrogenase
Mm03024075_m1	Hprt	hypoxanthine guanine phosphoribosyl transferase
Mm00813830_m1	Dagla	diacylglycerol lipase, alpha
Mm00515664_m1	Dio2	deiodinase, iodothyronine, type II
Mm00436590_m1	Slc1a1	solute carrier family 1, member 1
Mm01275814_m1	Slc1a2	solute carrier family 1, member 2
Mm00600697_m1	Slc1a3	solute carrier family 1, member 3
Mm01173279_m1	Slc1a6	solute carrier family 1, member 6
Mm00525562_m1	Slc1a7	solute carrier family 1, member 7
Mm00433753_m1	Gria1	glutamate receptor, ionotropic, AMPA1 (alpha 1)
Mm00442822_m1	Gria2	glutamate receptor, ionotropic, AMPA2 (alpha 2)
Mm00497506_m1	Gria3	glutamate receptor, ionotropic, AMPA3 (alpha 3)
Mm00444754_m1	Gria4	glutamate receptor, ionotropic, AMPA4 (alpha 4)
Mm00446882_m1	Grik1	glutamate receptor, ionotropic, kainate 1
Mm00599860_m1	Grik2	glutamate receptor, ionotropic, kainate 2 (beta 2)
Mm01179716_m1	Grik3	glutamate receptor, ionotropic, kainate 3
Mm00615472_m1	Grik4	glutamate receptor, ionotropic, kainate 4
Mm00433774_m1	Grik5	glutamate receptor, ionotropic, kainate 5 (gamma 2)
Mm00433790_m1	Grin1	glutamate receptor, ionotropic, NMDA1 (zeta 1)
Mm00433802_m1	Grin2a	glutamate receptor, ionotropic, NMDA2A (epsilon 1)
Mm00433820_m1	Grin2b	glutamate receptor, ionotropic, NMDA2B (epsilon 2)
Mm00439180_m1	Grin2c	glutamate receptor, ionotropic, NMDA2C (epsilon 3)
Mm00433822_m1	Grin2d	glutamate receptor, ionotropic, NMDA2D (epsilon 4)
Mm01341723_m1	Grin3a	glutamate receptor, ionotropic, NMDA3A
Mm00504568_m1	Grin3b	glutamate receptor, ionotropic, NMDA3B
Mm01187089_m1	Grm1	glutamate receptor, metabotropic 1
Mm01235831_m1	Grm2	glutamate receptor, metabotropic 2
Mm00725298_m1	Grm3	glutamate receptor, metabotropic 3

Mm01306128_m1	Grm4	glutamate receptor, metabotropic 4
Mm00690332_m1	Grm5	glutamate receptor, metabotropic 5
Mm00841148_m1	Grm6	glutamate receptor, metabotropic 6
Mm01189424_m1	Grm7	glutamate receptor, metabotropic 7
Mm00433840_m1	Grm8	glutamate receptor, metabotropic 8
Mm00443262_m1	TRHR1	thyrotropin-releasing hormone receptor 1
Mm01241598_m1	TRHR2	thyrotropin-releasing hormone receptor 2

Table S1. The table summarizes the assay ID, the symbol and the name of the genes included in the Custom TaqMan Gene Expression Array Cards that was used to investigate the presence and absence of glutamate transporters and glutamate receptor subunits in β-tanycytes. **Related to Table 1.**

The 18s ribosomal RNA, the actin beta (*Actb*), the glyceraldehyde-3-phosphate dehydrogenase (*Gapdh*) and the hypoxanthine-guanine phosphoribosyltransferase (*Hprt*) served as housekeeping genes. Diacylglycerol lipase alpha (*Dagla*) and *Dio2* served as positive controls.

Supplementary results

Presence of DAGLα in the tanycytes of the rat median eminence

Similarly to that observed in mice, DAGLα-immunoreactivity was observed in the cell bodies of tanycytes lining the ventricular wall of the median eminence (Fig. S1A) and the basal processes of these cells. The cell bodys of these tanycytes had, however, stronger DAGLα-immunoreactivity than the cell bodies of tanycytes in mice. In addition, the γ-tanycytes, that are located in the external zone of the median eminence (Wittmann et al., 2017), were strongly labeled with DAGLα-immunoreactivity (Fig. S1B)

Effects of NMDA and metabotropic glutamate receptor agonists on the β2 tanycytes of mice

As magnesium can block the NMDA receptors when the membrane potential is low, like the membrane potential of tanycytes, the effect of NMDA was also tested in voltage-clamp mode at -40 mV holding potential, where the NMDA receptors relieved from the magnesium block (Mayer et al., 1984). However, NMDA had no effect on the β2-tanycytes even under this condition (control: 6.14±7.58 pA, n=3 vs. 0.5 mM NMDA: 13.43±15.66 pA, n=3, P=1.00; Fig. S3) suggesting that the tanycytes do not have functional NMDA receptors.

Similarly, treatment of tanycytes with agonists of Type I (DHPG, used in mM: 0.1, 0.2, 1, 2 and 2.5; n=6), Type II (APDC, used in mM: 0.2, 2 and 2.5; n=5) metabotropic glutamate receptors had no effect on the membrane potential of β2-tanycytes (Fig. S3).

Grm1 and Grm5 mRNA levels are under the detection limit in tanycytes

While high level of Grm1 and Grm5 mRNA are detectable in the neuropil around the third ventricle, silver grains denoting the in situ hybridization signal were not observed above the cell bodies of tanycytes (Fig. S4).

Transparent Methods

Animals

Adult, male CD1 mice weighing 28-32 g were used for the morphological studies. Male C57Bl/6J mice between P40 and P60 days of age were used for *in vitro* patch clamp electrophysiology studies. Adult, male TRH-IRES-Cre mice between P55 and P70 days of age were used for the optogenetic studies. Rax/CreERT2//Gt(ROSA)26Sor_CAG/LSL_ZsGreen1 were used in studies examining the presence of DAGLα in the β-tanycytes in mice. DAGLα mice were used to demonstrate the DAGLα-immunoreactivity in the median eminence. Mice were housed under standard conditions (lights on between 06.00 and 18.00 h, temperature 22±1 °C, chow and water *ad libitum*). All experimental protocols were reviewed and approved by the Animal Welfare Committees at the Institute of Experimental Medicine of the Hungarian Academy of Sciences.

Male Wistar rats P80 days old, raised as an outbred colony at the Institute of Biotechnology, UNAM, and 250g male Sprague-Dawley rats from AnimaLab Hungary Kft. (Budapest, Hungary) were used for median eminence explant experiments and study the presence of DAGLα-immunoreactivity in the tanycytes of rats. They were kept under controlled temperature (20-22 °C), lights on from 7:00 to 19:00 h, with water and food (Harlan 2018S) *ad libitum*.

All experimental protocols were reviewed and approved by the Animal Welfare Committee at the Institute of Experimental Medicine of the Hungarian Academy of Sciences or by the Bioethics Committee of the Institute of Biotechnology, UNAM.

Generation of the TRH-IRES-Cre mouse line

An IRES Cre-recombinase cassette was inserted into the mouse TRH locus using CRISPR/Cas9 on an FVB.129P2-Pde6b^{+} Tyr$^{c\text{-}ch/}$AntJ (FVB/Ant) background. This was performed by the

modification of the targeting construct that was recently used to create the TRH-IRES-tdTomato mouse using 1473 bp long 5' and the 1375 bp long 3' TRH arms (Varga et al., 2019). The targeting construct was cut with by EcoRI and NotI to remove the TdTomato cassette. A Nuclear Localization Signal (NLS) containing Cre-recombinase encoding cassette was generated with Vent PCR on a Turbo-Cre plasmid (kindly porvided by Dr Ley (Revell et al., 2005)). (sense oligo: ggaattcactATGCCCAAGAAGAAGAGGAAGGTGTCCAATT; antisense oligo: ataagaatgc ggccgc CTAATCGCCATCTTCCAGCAGGCGCA) followed by the insertion of the NLS-Cre cassette between EcoRI and NotI of the targeting construct. The construct was confirmed by sequencing.

Pronuclear microinjection was carried out on fertilized eggs of FVB/Ant mice, using of a single guide RNA with the target sequence of GGAGTAAGGTTAGAGTC and Cas9 mRNA (Trilink).

Founders were identified with PCR checking the insertion with outer and inner PCR oligos (outer antisense: CTTCCATGAGAGGAGTATTTATCA; NLS-Cre sense1: GCTGGAAGATGGCGATTAG; NLS-Cre sense2: GAAGCAACTCATCGATTGATT).

A founder with a single copy of the targeting cassette was selected for breeding.

Heterozygote F1 animals were crossbred with littermate animals of identical genotype. Mice were bred and maintained as homozygous colonies.

Tissue fixation and preparation for morphological studies

For morphological studies the animals were anaesthetized with a mixture of ketamine and xylazine (ketamine 50 mg/kg, xylazine 10 mg/kg body weight, i.p.) and perfused transcardially with fixative solution. The details of tissue fixation and tissue preparation are described below.

For *in situ* hybridization (N=4), mice were perfused transcardially with 10 ml 0.01 M phosphate-buffered saline pH 7.4 (PBS), followed by 50 ml 4% paraformaldehyde in 0.1 M

phosphate buffer pH 7.4 (PB) (all solutions were RNAse-free). The brains were rapidly removed and were cryoprotected in 20% sucrose in 0.01 M PBS overnight at 4 ^{o}C. The brains were then snap frozen with powdered dry ice and stored at -80 ^{o}C until used.

For light microscopy, the anaesthetized mice (N=9) and rats (N=3) were perfused transcardially with 10 ml 0.01 M PBS, followed by 50 ml 4% paraformaldehyde in 0.1M PB or by 150 ml 4% paraformaldehyde in 0.1M PB, respectively. The brains were rapidly removed and were cryoprotected in 30% sucrose in 0.01 M PBS overnight at room temperature (RT). The brains were then snap frozen with powdered dry ice and stored at -80 ^{o}C until used.

For electron microscopy (N=3), the anaesthetized animals were perfused transcardially with 10 ml 0.01 M PBS, followed by 50 ml 4% acrolein in 2% paraformaldehyde in 0.1 M PB.

For light microscopic immunocytochemistry or for immunofluorescence, serial, 25 µm thick coronal sections were cut through the median eminence (ME) using freezing microtome (Leica Microsystems, Wetzlar, Germany). Series of sections, obtained at 100 µm intervals, were collected into antifreeze solution (30% ethylene glycol; 25% glycerol; 0.05 M PB) and stored at -20 °C until their use for immunohistochemistry. The sections were then pretreated first with 0.5% Triton X-100 and 0.5% H_2O_2 in 0.01 M PBS for 15 min. Nonspecific antibody binding was blocked with treatment in 2% normal horse serum (NHS) in PBS for 20 min at room temperature (RT).

For ultrastructural studies, serial 25 µm thick coronal sections were cut on a Leica VT 1000S vibratome (Leica Microsystems, Wetzlar, Germany) through ME. The sections were treated with 0.5% H_2O_2 in PBS for 15 min, cryoprotected in 15% sucrose in PBS for 15 min at RT and in 30% sucrose in PBS overnight at 4 °C. Then, the sections were quickly frozen over liquid nitrogen and thawed. This cycle was repeated three times to improve antibody penetration.

Single-labeling immunocytochemistry for DAGLα

One-in-four series of sections from each brain and sections from 2 DAGLα mice were incubated in guinea-pig anti DAGLα serum (Keimpema et al., 2013) at 1:500 dilutions in 2% NHS overnight at RT. Then, sections were incubated in a biotinylated donkey anti guinea-pig IgG (1:500, Jackson) in 2% NHS for 2 h. After washing steps in PBS and treatment with avidin-biotin-peroxidase complex (ABC 1:1000, Vector lab, Vectastain kit), the DAGLα-immunoreactivity was detected in Ni-DAB developer (0.05% DAB/0.15% Ni-ammonium-sulfate/0.005% H_2O_2 in 0.05 M Tris buffer, pH 7.6). Then, the sections were mounted onto glass slides and coverslipped with DPX mounting medium (Sigma). Immunoreaction signal was completely absent from the ME of DAGLα mice.

Detection of DAGLα-immunoreactivity in the tanycytes of the ME in mice and rats

To detect the tanycytes in the median eminence of mice Rax/CreERT2 mice (Gift from Dr Blackshaw (Pak et al., 2014)) were crossed with Gt(ROSA)26Sor_CAG/LSL_ZsGreen1 mice (Jackson Laboratoratory, Bar Harbor, ME). The ZsGreen1 expression of tanycytes was induced in the resulted double transgenic Rax/CreERT2//Gt(ROSA)26Sor_CAG/LSL_ZsGreen1 mice by tamoxifen treatment. Tamoxifen (175 mg/kgBW) dissolved in corn oil was administered daily for 4 days by oral gavage. The day after the last tamoxifen treatment, the mice were anaesthetized, perfused transcardially with 4% PFA and the brains were sectioned with freezing microtome as described above. After pretreatment, one-in-four series of sections from each brain were incubated in rabbit anti-DAGLα antibody (Katona et al., 2006) in 2µg/ml concentration overnight at RT. Then the sections were incubated in Alexa 555-conjugated donkey anti rabbit IgG (1:500, Invitrogen) for 2h, mounted onto glass slides and coverslipped with Vectashield mounting medium (Vector).

To detect the tanycytes in the median eminence of rats, one-in-four series of sections from each brain were incubated in a mixture of rabbit anti-DAGLα antibody (Katona et al., 2006) in 2µg/ml concentration and goat anti vimentin antibody (Santa Cruz Biotech) at 1:3000 dilution overnight at RT. Then the sections were incubated in a mixture of Alexa 555-conjugated donkey anti rabbit IgG (1:500, Invitrogen) and Alexa 488-conjugated donkey anti sheep IgG (1:500, Invitrogen) for 2h, mounted onto glass slides and coverslipped with Vectashield mounting medium (Vector). Nikon A1R confocal microscope was used for imaging.

Triple-labeling immunofluorescence for CB1, DAGLα and TRH

One-in-four series of sections from each brain were incubated in goat anti-CB1 antibody at 1:1000 dilution (Makara et al., 2007), guinea-pig anti-DAGLα antibody (Malenczyk et al., 2015) at 1:500 and rat anti-mouse proTRH 178-200 serum (Peterfi et al., 2018) at 1:250 in 2% NHS overnight at RT. Then, the sections were incubated in biotinylated donkey anti guinea-pig IgG (1:500) for 1 h, at RT followed by incubation in a mixture of Streptavidin conjugated cy5 (1:250, Jackson), Alexa 555 conjugated donkey anti-sheep IgG (1:500, Invitrogen) and Alexa 488 conjugated donkey anti-rat IgG (1:250, Invitrogen) for 2 h, mounted onto glass slides and coverslipped with Vectashield mounting medium (Vector). Images were taken using Zeiss LSM 780 confocal microscope (Zeiss Company, Jena, Germany) using line by line sequential scanning with laser excitation lines 410-483 nm for Dylight 405, 490-553 nm for Alexa Fluor 488 and 566-697 nm for Alexa Fluor 555; beamsplitter/emission filters, MSB 405 nm for Alexa Fluor 405, MSB488/561 nm for Alexa Fluor 488 and Alexa Fluor 555. For 40x and 60x oil lenses, pinhole sizes were optimized resulting in 0.9 µm thin optical slices, respectively. The series of optical sections were recorded with 0.7 µm Z steps. Images were analyzed with Zen 2012 (Zeiss Company, Jena, Germany) and with Adobe Photoshop (Adobe System Inc., California, US.).

Single-labeling immuno-electron microscopy using silver-intensified Ni-DAB chromogen

One-in-four series of pretreated sections from each brain were incubated in guinea-pig anti DAGLα serum at 1:500 dilution in 2% NHS for 4 days at 4 °C. After rinsing in PBS, the sections were incubated in biotinylated donkey anti-guinea-pig IgG (1:500, Jackson) diluted in 2% NHS for 2 h at RT, followed by treatment in ABC (1:1000, Vector lab). The DAGLα-immunoreactivity was NiDAB developed. The resultant reaction product was silver-gold-intensified using the Gallyas method (Liposits et al., 1982). The sections were osmicated for 1h at RT, and then treated with 2% uranyl acetate in 70% ethanol for 30 min. Following dehydration in an ascending series of ethanol and acetonitrile (Sigma Aldrich), the sections were flat embedded in Durcupan ACM epoxy resin (Sigma Aldrich) on liquid release agent (Electron Microscopy Sciences) coated slides and polymerized at 56 °C for 2 days. After polymerization, 60–70 nm thick ultrathin sections were cut with Leica ultracut UCT ultramicrotome (Leica Microsystems, Wetzlar, Germany). The ultrathin sections were mounted onto Formvar-coated, single slot grids, contrasted with 2% lead citrate (Sigma Aldrich, Hungary) and examined with a JEOL-100 C transmission electron microscope.

Specificity of the antibodies

The specificity of the goat anti-CB1 antibody was proved in CB1 KO animals (Hajos et al., 2000), and the specificity of the rat anti-mouse proTRH 178-200 serum was demonstrated by double labeling immunofluorescence showing that the rat anti-mouse proTRH 178-200 antiserum and the sheep TRH antiserum had identical distribution (Peterfi et al., 2018). The specificity of the guinea-pig anti-DAGLα serum was established by the complete absence of the immunoreaction signal in the median eminence of mice when sections of DAGLα knock-out mice (Tanimura et al., 2010) were used.

Double labeling in situ hybridization for TRH and CB1 mRNAs

Coronal, 20 µm thick sections were cut with a cryostat (Leica) through the antero-posterior extent of the PVN. The sections were collected in an RNAse free cryoprotective solution (30% ethylene glycol; 25% glycerol; 0.05 mM PB) and stored at -20 °C until use.

Serial sections were washed in 2× SSC, acetylated with 0.25% acetic anhydride (Sigma-Aldrich) in 0.9% triethanolamine (Sigma-Aldrich) for 20 min. To facilitate the penetration of labeled RNA probes, the sections were delipidated by treatment in 50%, 70% and again 50% acetone (Sigma-Aldrich). After additional washes in 2×SSC for 5 min, the sections were hybridized with the mixture of digoxigenin-labeled cRNA probe for proTRH and [35S]UTP-labeled cRNA probe for CB1.

The hybridization was performed for 16 h at 56 °C in 200 µl polypropylene tubes in a hybridization buffer (50% formamide, 2× SSC, 10% dextran sulfate, 0.5% SDS, and 250 µg/ml denatured salmon sperm DNA) that contained the digoxigenin-labeled proTRH probe diluted 1:50 and 50000 cpm/µl of [35S]-labeled CB1 cRNA probe. The sections were washed in 1× SSC for 15 min and then treated with 25 µg/ml RNase for 1 hour at 37 °C. After additional washes in 0.1× SSC (four times for 15 min) at 65 °C, sections were washed in PBS, treated with a mixture of 0.5% Triton X-100 and 0.5% H_2O_2 for 15 min, and then treated with 2% bovine serum albumin (BSA) in PBS for 20 min to reduce the nonspecific antibody binding. The sections were incubated with sheep anti-digoxigenin-peroxidase Fab fragments (1:100; Boehringer Mannheim Corp., Indianapolis, IN) in 1% BSA in PBS overnight at 4 °C. The sections were then rinsed in PBS and incubated in 0.1% biotinylated tyramide and 0.01% H_2O_2 in PBS for 10 min to intensify the hybridization signal. After additional washes, the sections were incubated in streptavidin conjugated Alexa 555 (1:250; Vector Laboratories, Burlingame, CA) and mounted on gelatin coated glass slides. The slides were dipped into Kodak NTB

autoradiography emulsion (Eastman Kodak, Rochester, NY), and the autoradiograms were developed after 3 weeks of exposure at 4 °C. The specificity of hybridization was confirmed using sense probes, which resulted in the absence of specific hybridization in the paraventricular nucleus (PVN).

Both sides of the PVN from three sections of each brain containing the mid-level of PVN were imaged with a Zeiss AxioImager M1 microscope equipped with MRC5 digital camera (Carl Zeiss) using a 20X objective. Both darkfield and epifluorescent images of the same field were taken. The images were overlaid in Adobe Photoshop CS5 software (Adobe Systems Inc.). The ratio of red fluorescent TRH neurons that had accumulation of silver grains were counted.

Determination of the role of the endocannabinoid system in the regulation of TRH release in the ME

To understand the effects of endocannabinoids on the TRH release of median eminence explants, a total of 70 WISTAR rats were used in two independent experiments. Rats were individually transported from their nearby house-room to the procedural room and decapitated, by an experienced technician, with a sharp guillotine; between each killing the area was thoroughly cleaned. Each brain was excised from skull, taking care first to cut the optic nerve to preserve ME intact. Under a stereo microscope, the ME together with part of the arcuate nucleus was dissected. Explants were incubated as described (Joseph-Bravo et al., 1979) with the following modifications: two explants were placed together in a microcentrifuge tube containing 300 µl of Hank's solution saturated with 95% O_2/5% CO_2, kept at 4 ^oC until end of dissections (max. 40 min); medium was then replaced with 200 µl fresh artificial CSF medium (ACSF) saturated with 95% O_2/5% CO_2 containing in mM: 125 NaCl, 2.5 KCl, 25 glucose, 25 $NHCO_3$, 1.25 NaH_2PO_4, 2 $CaCl_2$, 1 $MgCl_2$, pH 7.4 and 200 nM of a phosphinic analogue of TRH (GlpΨ[P(O)(OH)]HisProNH2; P-TRH), a TRH-DE inhibitor (Matziari et al., 2008).

Explants were pre-incubated at 37 ºC for 10 min. After preincubation, medium was replaced with 200 µl of ACSF-P-TRH and the drugs (Sigma-Aldrich) under study: CB1 antagonist, AM125 at 1 µM (Kola et al., 2008); CB1 agonist, WIN55,212-2 at 1 µM (Farkas et al., 2010); DAGLα inhibitor, tetrahydrolipstatine (THL) at 10 µM (Farkas et al., 2010); either alone or combined as stated in Fig. 2; control medium was ACSF-P-TRH. Drugs were initially dissolved in DMSO (final concentration: 0.0025%). Explants were incubated for 10 min at 37 ºC; then, 170 µl of medium were recovered into 800 µl of cold methanol. Another 200 µl of ACSF-P-TRH and respective drug was added and the explants incubated 10 more min at 37 ºC; afterwards a 170 µl aliquot of medium was recovered into 800 µl of cold methanol. Tubes containing medium/methanol were kept overnight at -20 °C, centrifuged at 12100 g for 30 min at 4 ºC and supernatant evaporated. Residues were resuspended in 90% methanol, kept overnight at -20 °C, centrifuged, supernatant evaporated and TRH quantified by radioimmunoassay (RIA) using the R2 antibody (Joseph-Bravo et al., 1979). The amount of TRH detected in the two subsequent incubates was added, and the average quantity detected in control tubes considered 100%; each value was calculated as % of control. The explant was recovered and extracted as reported to determine the residual intracellular level of TRH (Joseph-Bravo et al., 1979).

Determination of the role of endogenous glutamate in the regulation of 2-AG content of the ME

To elucidate the effect of glutamate on the 2-AG content of the median eminence, 14 Sprague-Dawley rats were used. ME explants were prepared as described above. One explant was placed in each microcentrifuge tube containing 300 µl of Hank's solution saturated with 95% O_2/5% CO_2, kept at on ice until end of dissections (max. 40 min); medium was then replaced with 200

µl fresh ACSF saturated with 95% O_2/5% CO_2. Explants were pre-incubated at 37 ^oC for 10 min. After preincubation, medium was replaced with 200 µl of ACSF+1%DMSO or 200 µl of ACSF+1% DMSO containing the mixture 500 µM DNQX and 1mM TBOA to block the effects of glutamate on the tanycytes. After 10 min incubation, 170µl solution was removed and replaced with 200µl similar solution. All solutions were saturated with 95% O_2/5% CO_2.

After additional 10 min incubation, all solutions were removed and the ME samples were frozen on powdered dry ice.

To measure endocannabinoid levels, we used a PerkinElmer Life and Analytical Sciences HPLC Series 200 system, which was coupled to an Applied Biosystems/Sciex 4000 QTRAP triple quadrupole/linear ion trap tandem mass spectrometer operated in positive electrospray ionization mode. The electronspray ionization ion source parameters were set as follows: curtain gas, 10; ion spray voltage, 5000 V; temperature, 500°C; collisionally activated dissociation gas, medium; gas 1, 50; gas 2, 40. Chromatographic separation was achieved with a Phenomenex Kinetex C18 column (50mmx3.00 mm) using methanol and 10 mM ammonium formate as elution solvents at a flow rate of 500 l/min. The injection volume was 50 µl. The initial eluent condition was 80% methanol/20% buffer that was increased to 85% organic phase during 3 min and then further elevated to 95% during 2 min and was kept at this condition for 2 min. Afterward, the column was equilibrated to the initial condition. Analytes were detected in multiple reaction monitoring (MRM) mode at the following ion transitions and parameter settings: (1) 2-AG, MRM transition [mass/charge ratio (m/z), 379.4 - 287.2, 379.4 - 91.1], declustering potential (81 V), collision energy (23 V, 81 V), cell exit potential (10 V, 8 V); (2) 2-arachidonoylglycerol-d5, MRM transition (m/z, 384.4 - 287.2, 384.4 - 91.1), declustering potential (81 V), collision energy (23 V, 81 V), cell exit potential (10 V, 8 V). The peak areas were determined with Analyst 1.4.2. software. The quantity of the analytes was calculated by comparing their peak areas with those of the deuterated internal standards, and it was

normalized to the sample weight. All endocannabinoid standards were purchased from Cayman Chemical. HPLC gradient-grade methanol was supplied by Merck. Ammonium formate was from Sigma. Water was purified with a MilliQ Direct 8 system (Millipore).

Sample preparation for chromatography started with tissue incubation on ice for 5 min in 100 µl of methanol containing the deuterated internal standards 2-arachidonoylglycerol- d5 (100 ng/ml). After ultrasonic homogenization, samples were centrifuged on an Eppendorf miniSpin microtube centrifuge at 13,400 rpm for 15 min. The supernatants were diluted to initial HPLC eluent composition with 10 mM ammonium formate solution.

In situ hybridization detection of Grm1 and Grm5 mRNAs

Serial, 12 µm thick coronal sections of fresh frozen brains of adult male CD1 mice were cut with a cryostat (Leica Microsystems GmbH, Wetzlar, Germany) through the antero-posterior extent of the median eminence. The sections were mounted on Superfrost Plus slides (Fisher, Hampton, NH), and dried at 42 ^{o}C overnight, as described (Hrabovszky and Petersen, 2002). On the day of hybridization, the sections were fixed with 4% paraformaldehyde in PBS (pH 7.4) for 1 h, washed in 2-fold concentration of standard sodium citrate (2× SSC), acetylated with 0.25% acetic anhydride in 0.9% triethanolamine for 20 min, and then treated in graded solutions of ethanol (70, 80, 96, and 100%), chloroform, and a descending series of ethanol (100 and 96%) for 5 min each, and hybridized with *Grm1* or *Grm5* single-stranded ^{35}S-UTP labeled cRNA probes. The hybridizations were performed under plastic coverslips in a buffer containing 50% formamide, 2-fold concentration of SSC (2× SSC), 10% dextran sulfate, 0.5% sodium dodecyl sulfate, 250 µg/ml denatured salmon sperm DNA, and $5x10^4$ cpm/µl radiolabeled probe for 16 h at 56 ^{o}C. The slides were washed in 1× SSC for 15 min and then treated with RNase (25 µg/ml) for 1 h at 37 ^{o}C, followed by additional washes in 0.1× SSC (2

× 30 min) at 65 ºC. After dehydration in graded dilutions of ethanol, the slides were dipped into Kodak NTB autoradiography emulsion (Eastman Kodak, Rochester, NY), and the autoradiograms were developed after 6-wk exposure at 4 ºC. The specificity of hybridization was confirmed using sense probes that resulted in the complete absence of hybridization signal in the brain. Sections were immersed in 0.0005% cresyl violet acetate (Sigma-Aldrich) for 2 minutes to obtain fluorescent labeling of cell nuclei, dehydrated in ascending ethanol series and xylenes, and coverslipped with DPX mountant (Alvarez-Buylla et al., 1990).

Examination of the glutamate receptor and transporter expression in β-tanycytes

Adult, male, CD1 mice were transcardially perfused with ice-cold 10% RNAlater solution (Ambion) diluted in DEPC treated 0.1M PBS. Brains were quickly removed and placed into -35-40 °C cold 2-methylbutane (Sigma-Aldrich), cooled down with a mixture of 100% ethanol and dry ice. Brains were kept in -80 °C freezer until sectioning.

12 µm coronal brain sections were cut at -18 °C using a cryostat (Leica, Germany). Sections were mounted on PEN-membrane slides (Zeiss, Germany), thawed and counterstained with 0.6% cresyl violet dissolved in 70% ethanol. Then, the sections were dehydrated in a series of ascending ethanol and stored at -80 °C until further processing.

The sections were thawed under vacuum and the cell bodies of β-tanycytes lining the floor of the third ventricle were microdissected using Zeiss Microbeam Laser Capture Microdissection (LCM) system and PALM software. The β-tanycyte samples were pressure-catapulted with a single laser pulse into 0.5 ml adhesive cap tubes (Carl Zeiss Microimaging) using a ×20 objective lens.

RNA isolation was performed from the isolated β-tanycytes using Arcturus PicoPure RNA Isolation Kit (Applied Biosystems). To remove potential genomic DNA contamination, DNase treatment was carried out on the RNA purification column using RNase-Free DNase Set (Qiagen). The quality and the concentration of the isolated RNA samples were measured with

Bioanalyzer using Agilent RNA 6000 Pico Kit and 2100 Expert software (Agilent Technologies).

The RNA samples were transcribed using ViLO Superscript III cDNA Reverse Transcription Kit (Invitrogen) according to the manufacturer's protocol. The cDNA concentration was measured with Qubit® Fluorometer by using Qubit® ssDNA Assay Kit (Invitrogen). The cDNA product served as a template for preamplification by using Preamp Master Mix Kit (Applied Biosystems) and the double stranded DNA concentration was measured with Qubit® Fluorometer using the Qubit® dsDNA BR Kit (Invitrogen).

384-well Custom TaqMan® Gene Expression Array Cards (Applied Biosystems) were used to identify the expression of glutamate receptor subunits and glutamate transporters in the β-tanycytes. The microfluidic card was preloaded by the manufacturer with selected gene expression assays for our target receptors, transporters and housekeeping genes listed in Supplementary Table 1. ViiA 7 real-time PCR platform with Array Card Block and comparative CT method (Life Technologies) was used for thermal cycles of the qPCR.

The 18s ribosomal RNA, the actin beta (*Actb*), the glyceraldehyde-3-phosphate dehydrogenase (*Gapdh*) and the hypoxanthine-guanine phosphoribosyltransferase (*Hprt*) served as housekeeping genes, namely, the CT values of each genes of our interest were normalized to the CT value of the geometric mean of these housekeeping genes. *Dio2* is known to be expressed by tanycytes (Fekete et al., 2000, Tu et al., 1997), and our current immunocytochemical data showed that diacylglycerol lipase alpha (*Dagla*) is also expressed in tanycytes, thus, these genes served as positive controls. As our in situ hybridization studies demonstrated that the metabotropic glutamate receptor 5 (*Grm5*) and the metabotropic glutamate receptor 1 *(Grm1)* are not expressed in tanycytes (Supplementary Fig. 4), the expression levels of these genes were used as a threshold value. Thus, genes that had CT value

equal or lower than that of *Dagla* were considered to be expressed in β-tanycytes, while genes above the threshold of the CT values of *Grm5* were considered to be absent in β-tanycytes.

Slice preparation for electrophysiological recordings

The mice were deeply anaesthetized with isoflurane and decapitated. The brains were rapidly removed and immersed in ice-cold slicing solution containing, in mM: 87 NaCl, 2.5 KCl, 0.5 $CaCl_2$, 7 $MgCl_2$, 25 $NaHCO_3$, 25 D-glucose, 1.25 NaH_2PO_4, 75 sucrose saturated with 95% O_2/5% CO_2. Coronal 250 µm slices were cut using a VT1200S vibratome (Leica), then the slices were transferred into a holding chamber filled with artificial cerebrospinal fluid (aCSF; 36 °C) containing in mM: 126 NaCl, 2.5 KCl, 26 $NaHCO_3$, 2 $CaCl_2$, 2 $MgCl_2$, 1.25 NaH_2PO_4, 10 glucose; pH 7.4; 280-300 mOsm/L. The slices were kept in holding solution for at least 1.5 hours and gradually cooled down to room temperature.

Chemicals used for electrophysiology

The chemicals for the intracellular and extracellular solutions, carbenoxolone disodium salt (carbenoxolone) and L-Glutamic acid (glutamate) were purchased from Sigma-Aldrich. Tetrodotoxin (TTX), (2S,3S,4S)-Carboxy-4-(1-methylethenyl)-3-pyrrolidineacetic acid (kainate), (RS)-α-Amino-3-hydroxy-5-methyl-4-isoxazolepropionic acid (AMPA), N-Methyl-D-aspartic acid (NMDA), 6,7-Dinitroquinoxaline-2,3-dione disodium salt (DNQX) (S)-3,5-Dihydroxyphenylglycine (DHPG), (2R,4R)-4-Aminopyrrolidine-2,4-dicarboxylate (APDC), L-(+)-2-Amino-4-phosphonobutyric acid (L-AP4) and DL-threo-β-Benzyloxyaspartic acid (TBOA), Vu 155041 were purchased from the Tocris Bioscience. TBOA was dissolved in dimethylsulfoxide (DMSO) and then diluted in aCSF. The final concentration of DMSO used in the experiments was <0.01%. TRH was purchased from Bachem (Switzerland).

Data acquisition and analysis for electrophysiology

The slices were transferred to a submersion type of recording chamber containing aCSF at 32-33 °C and were perfused with aCSF at a rate of approximately 1 mL/min. As tanycytes express connexin 43 gap junctions and hemichannels (Szilvasy-Szabo et al., 2017), gap junction inhibitor carbenoxolone (100 μM) was added to the aCSF to block the intercellular communication *via* gap junctions. To prevent the potential indirect effects of glutamate treatment, the voltage-dependent sodium channel inhibitor, TTX (600 nM) was also continuously administered into the aCSF. β2-tanycytes were identified based on their typical morphology and the location of their cell body in the floor of the third ventricle under infrared differential interference contrast illumination using FN1 Microscope (Nikon) equipped with 40x water-immersion objective with additional zoom (up to 2x) and Zyla CCD camera (ANDOR). The patch pipettes (6-8 MΩ) were pulled from borosilicate capillaries (OD=1.5 mm thin wall, Garner Co.) with a P-1000 horizontal puller (Sutter Instrument Co.) and filled with intracellular recording solution containing, in mM: 110 K-gluconate, 4 NaCl, 20 HEPES, 0.1 EGTA, 10 phosphocreatine di(tris) salt, 2 ATP, 0.3 GTP; pH 7.25; 280-300 mOsm/L. Recordings were performed with Multiclamp 700B patch clamp amplifier, Digidata-1440A data acquisition system and pCLAMP 10.4 software (Molecular Devices). The headstage of the amplifier was fitted to a Luigs&Neumann SM7 micromanipulator system. Whole-cell and outside-out patch-clamp recordings were filtered at 10 kHz using the built-in Bessel filter of the amplifier and digitized at 10 kHz. Slow and fast capacitive components were automatically compensated for. The stability of the patch was checked by repetitively monitoring the access resistance during the experiment. Liquid junction potential was 14.4 mV and not compensated.

Whole-cell patch clamp recording

The membrane potential (MP) was measured immediately after break-in and establishing whole-cell recording in current-clamp mode (I=0). In each series of experiments, a control period was recorded for 2-3 min that was followed by a drug treatment phase for 3-4 min. During the treatment, the perfusion was opened. The final volume of the drug was 300 μL and the treatment lasted until this volume passed through the recording chamber. The concentration of the drug used in the recording chamber is described in the Results section. The effect of the drugs was examined on the MP of β2-tanycytes. The washout of the drugs restored the MP of β2-tanycytes in all cases.

Outside-out patch clamp recording

To exclude the indirect effect of substances that may be released from neighboring non-neuronal cells, the effect of glutamate was examined using outside-out patch clamp preparations. After establishing stable, whole-cell patch clamp connection, β2-tanycytes were isolated from the tissue by pulling them into the third ventricle. The MP was held at -78 mV and the inward current was measured during glutamate treatment (500 μM).

Examination of the influence of optogenetic activation of the hypophysiotropic TRH axon terminals on the membrane potential of tanycytes

The AAV5.EF1a.DIO.hChR2(H134R)-eYFP.WPRE.hGH virus (Addgene 20298P) was bilaterally injected into the PVN of 19 TRH-IRES-Cre mice. The surgeries were performed in a biosafety level 2 (BSL-2) virus injection facility. The mice were anesthetized (intraperitoneal injection of 25mg/kg xylazine and 125mg/kg ketamine in 0.9% NaCl) and their head positioned in a stereotaxic apparatus (Kopf Instruments, Tujunga, CA, USA) with the Bregma and Lambda in the horizontal plane. Through burr holes in the skull, a glass pipette (20-μm outer tip

diameter) connected to a Nanoject II/Nanoliter 2000 microinjector (Drummond Scientific Co. or WPI Inc.) was lowered into the brain at stereotaxic coordinates corresponding to the two sides of the PVN (anteroposterior: -0.7 mm, mediolateral: + or -0.3mm, dorsoventral: -5.0 mm) based on the atlas of Paxinos and Watson (Paxinos and Watson, 1998). The virus containing solution was injected bilaterally into the PVN 20nl with 100nl/min and another 30nl with 57nl/sec speed. Three minutes after the injections, the pipettes were removed slowly, the scalp was sutured and the mice were housed in BSL-2 quarantine for 2 weeks. Then the animals were used within two weeks.

On the day of the experiment, the mice were sacrificed and slices were prepared for electrophysiology as described above. B2-tanycytes were patched and their membrane potential was measured as described above. Carbenoxolone (100 μM) was added to the aCSF to block the intercellular communication *via* gap junctions. To activate the channelrhodopsin-containing TRH axons in the external zone of the ME, a micromanipulator-attached fibre optic cable (200 μm core diameter) delivered light from a laser (473 nm, Roithner Lasertechnik GmbH, Wien, Austria) The fiber optic was placed 1–2 mm away from the target area. Light intensity was calibrated by a Handheld Laser Power Meter (Edmund Optics; Nether Poppleton, York, UK). Maximally, 2.5 mW light was delivered to the tissue. The blue light was delivered in 2ms pulses at a 10 Hz frequency in 0.1s sweeps. The membrane potential changes were measured with Clampfit v10.7 using the average of 10 sweeps. In some of the cells, the effect of photostimulation was also studied in the presence of glutamate receptor (DNQX, 500 μM) and glutamate transporter inhibitors (TBOA, 1mM).

To determine whether the blue laser light can directly influence the tanycytes, control experiment was performed using slices of TRH-IRES-tdTomato mice where the TRH axons contained the tdTomato fluorescent protein.

Calcium imaging of tanycytes

Coronal slices (250 μm thick) containing intact ME were incubated with Fluo-4 AM (20 μM; Invitrogen) dissolved in extracellular solution containing low glucose (aCSF containing 1 mM glucose and 9 mM sucrose), DMSO (0.125% final concentration; Invitrogen), and Pluronic F-127 (0.05% final concentration; Invitrogen). Dye was allowed to diffuse into the tanycytes for at least 60-90 min before starting calcium imaging. Incubation of sections and calcium imaging experiments were carried out at room temperature to decrease intracellular compartmentalization of the dye. Despite the long incubation period, only few β2-tanycytes (3-8 cells) were loaded with dye, while almost all α-tanycytes cells were labelled.

First, we recorded a stabile baseline for 1 min without any treatment. This is considered as control period, then drugs were directly pipetted into the recording chamber and recording was continued for another 2-4 min. Tanycytes that did not show stable FIV during the control (baseline) period were excluded from analyses.

Andor AMH-200-FS6 halide light source was used to illuminate the sections. Fluorescence signal was collected, using a Nikon 40× objective lens, and images were collected at a 0.5 Hz sampling rate with 200 ms exposure time using an Andor Zyla 5.5 camera (Andor Technology, UK) equipped with an optical sectioning device (DSD2, Andor Technology, UK) to generate semi-confocal images. All semi-confocal image data were collected and analyzed using Nikon control and analysis software (NIS-Elements AR 4,40 64 bit versions).

Statistical analyses

Changes of the MP and inward current were analyzed using Clampfit module of the pCLAMP 10.4 software (Molecular Devices) and OriginPro 2015. Statistical tests were performed using one-way analysis of variance (ANOVA) followed by the Bonferroni correction to determine differences among treatment groups in the dose-response and mGLU4 agonist experiment and

ANOVA with repeated measure followed by the Bonferroni correction for all other patch clamp experiments. Treatment values were compared to their own control period. In calcium imaging recordings, nonparametric pairwise Wilcoxon test was carried out.

For TRH release of ME explants, significance was calculated by one-way ANOVA, followed by Tukey *post hoc* test, while the 2-AG content of ME explants was compared by Student's t-test. All data are reported as mean ± standard error of mean (SEM). The p value <0.05 was considered significant in all cases.

Supplementary References

Alvarez-Buylla, A., Ling, C. Y. & Kirn, J. R. (1990). Cresyl violet: a red fluorescent Nissl stain. J Neurosci Methods*,* 33**,** 129-33.

Farkas, I., Kallo, I., Deli, L., Vida, B., Hrabovszky, E., Fekete, C., Moenter, S. M., Watanabe, M. & Liposits, Z. (2010). Retrograde endocannabinoid signaling reduces GABAergic synaptic transmission to gonadotropin-releasing hormone neurons. Endocrinology*,* 151**,** 5818-29.

Fekete, C., Mihaly, E., Herscovici, S., Salas, J., Tu, H., Larsen, P. R. & Lechan, R. M. (2000). DARPP-32 and CREB are present in type 2 iodothyronine deiodinase-producing tanycytes: implications for the regulation of type 2 deiodinase activity. Brain Res*,* 862**,** 154-61.

Hajos, N., Katona, I., Naiem, S. S., Mackie, K., Ledent, C., Mody, I. & Freund, T. F. (2000). Cannabinoids inhibit hippocampal GABAergic transmission and network oscillations. Eur J Neurosci*,* 12**,** 3239-49.

Hrabovszky, E. & Petersen, S. L. (2002). Increased concentrations of radioisotopically-labeled complementary ribonucleic acid probe, dextran sulfate, and dithiothreitol in the hybridization buffer can improve results of in situ hybridization histochemistry. J Histochem Cytochem*,* 50**,** 1389-400.

Joseph-Bravo, P., Charli, J. L., Palacios, J. M. & Kordon, C. (1979). Effect of neurotransmitters on the in vitro release of immunoreactive thyrotropin-releasing hormone from rat mediobasal hypothalamus. Endocrinology*,* 104**,** 801-6.

Katona, I., Urban, G. M., Wallace, M., Ledent, C., Jung, K. M., Piomelli, D., Mackie, K. & Freund, T. F. (2006). Molecular composition of the endocannabinoid system at glutamatergic synapses. J Neurosci*,* 26**,** 5628-37.

Keimpema, E., Alpár, A., Howell, F., Malenczyk, K., Hobbs, C., Hurd, Y. L., Watanabe, M., Sakimura, K., Kano, M., Doherty, P., et al. (2013). Diacylglycerol lipase α manipulation reveals developmental roles for intercellular endocannabinoid signaling. Scientific Reports*,* 3**,** 2093.

Kola, B., Farkas, I., Christ-Crain, M., Wittmann, G., Lolli, F., Amin, F., Harvey-White, J., Liposits, Z., Kunos, G., Grossman, A. B., et al. (2008). The orexigenic effect of ghrelin is mediated through central activation of the endogenous cannabinoid system. PLoS One*,* 3**,** e1797.

Liposits, Z., Gorcs, T., Gallyas, F., Kosaras, B. & Setalo, G. (1982). Improvement of the electron microscopic detection of peroxidase activity by means of the silver intensification of the diaminobenzidine reaction in the rat nervous system. Neurosci Lett*,* 31**,** 7-11.

Makara, J. K., Katona, I., Nyiri, G., Nemeth, B., Ledent, C., Watanabe, M., De Vente, J., Freund, T. F. & Hajos, N. (2007). Involvement of nitric oxide in depolarization-induced suppression of inhibition in hippocampal pyramidal cells during activation of cholinergic receptors. J Neurosci*,* 27**,** 10211-22.

Malenczyk, K., Keimpema, E., Piscitelli, F., Calvigioni, D., Bjorklund, P., Mackie, K., Di Marzo, V., Hokfelt, T. G., Dobrzyn, A. & Harkany, T. (2015). Fetal endocannabinoids orchestrate the organization of pancreatic islet microarchitecture. Proc Natl Acad Sci U S A*,* 112**,** E6185-94.

Matziari, M., Bauer, K., Dive, V. & Yiotakis, A. (2008). Synthesis of the phosphinic analogue of thyrotropin releasing hormone. J Org Chem*,* 73**,** 8591-3.

Mayer, M. L., Westbrook, G. L. & Guthrie, P. B. (1984). Voltage-dependent block by Mg2+ of NMDA responses in spinal cord neurones. Nature*,* 309**,** 261-3.

Pak, T., Yoo, S., Miranda-Angulo, A. L., Wang, H. & Blackshaw, S. (2014). Rax-CreERT2 knock-in mice: a tool for selective and conditional gene deletion in progenitor cells and radial glia of the retina and hypothalamus. PLoS One*,* 9**,** e90381.

Paxinos, G. & Watson, C. 1998. *The Rat Brain in Stereotaxic Coordinates,* San Diego, CA, Academic Press.

Peterfi, Z., Farkas, E., Nagyunyomi-Senyi, K., Kadar, A., Otto, S., Horvath, A., Fuzesi, T., Lechan, R. M. & Fekete, C. (2018). Role of TRH/UCN3 neurons of the perifornical area/bed nucleus of stria terminalis region in the regulation of the anorexigenic POMC neurons of the arcuate nucleus in male mice and rats. Brain Struct Funct*,* 223**,** 1329-1341.

Revell, P. A., Grossman, W. J., Thomas, D. A., Cao, X., Behl, R., Ratner, J. A., Lu, Z. H. & Ley, T. J. (2005). Granzyme B and the downstream granzymes C and/or F are important for cytotoxic lymphocyte functions. J Immunol*,* 174**,** 2124-31.

Szilvasy-Szabo, A., Varga, E., Beliczai, Z., Lechan, R. M. & Fekete, C. (2017). Localization of connexin 43 gap junctions and hemichannels in tanycytes of adult mice. Brain Res*,* 1673**,** 64-71.

Tanimura, A., Yamazaki, M., Hashimotodani, Y., Uchigashima, M., Kawata, S., Abe, M., Kita, Y., Hashimoto, K., Shimizu, T., Watanabe, M., et al. (2010). The endocannabinoid 2-arachidonoylglycerol produced by diacylglycerol lipase alpha mediates retrograde suppression of synaptic transmission. Neuron*,* 65**,** 320-7.

Tu, H. M., Kim, S. W., Salvatore, D., Bartha, T., Legradi, G., Larsen, P. R. & Lechan, R. M. (1997). Regional distribution of type 2 thyroxine deiodinase messenger ribonucleic acid in rat hypothalamus and pituitary and its regulation by thyroid hormone. Endocrinology*,* 138**,** 3359-68.

Varga, E., Farkas, E., Zseli, G., Kadar, A., Venczel, A., Kovari, D., Nemeth, D., Mate, Z., Erdelyi, F., Horvath, A., et al. (2019). Thyrotropin-Releasing-Hormone-Synthesizing Neurons of the Hypothalamic Paraventricular Nucleus Are Inhibited by Glycinergic Inputs. Thyroid*,* 29**,** 1858-1868.

Wittmann, G., Farkas, E., Szilvasy-Szabo, A., Gereben, B., Fekete, C. & Lechan, R. M. (2017). Variable proopiomelanocortin expression in tanycytes of the adult rat hypothalamus and pituitary stalk. J Comp Neurol*,* 525**,** 411-441.